NISTIR 5357

Electronics and Electrical Engineering Laboratory

Technical Progress Bulletin

J. M. Rohrbaugh
Compiler

February 1994

Covering Laboratory Programs,
October to December 1993
with 1994/1995 EEEL Events Calendar

93-4

U.S. DEPARTMENT OF COMMERCE
Technology Administration
National Institute of Standards and Technology
Electronics and Electrical Engineering Laboratory
Semiconductor Electronics Division
Gaithersburg, MD 20899

NIST

NISTIR 5357

Electronics and Electrical Engineering Laboratory

J. M. Rohrbaugh
Compiler

U.S. DEPARTMENT OF COMMERCE
Technology Administration
National Institute of Standards and Technology
Electronics and Electrical Engineering Laboratory
Semiconductor Electronics Division
Gaithersburg, MD 20899

Technical Progress Bulletin

February 1994

Covering Laboratory Programs,
October to December 1993
with 1994/1995 EEEL Events Calendar

93-4

U.S. DEPARTMENT OF COMMERCE
Ronald H. Brown, Secretary

UNDER SECRETARY FOR TECHNOLOGY
Mary L. Good

NATIONAL INSTITUTE OF STANDARDS AND TECHNOLOGY
Arati Prabhakar, Director

ELECTRONICS AND ELECTRICAL ENGINEERING LABORATORY
TECHNICAL PROGRESS BULLETIN, FEBRUARY 1994 ISSUE

INTRODUCTION

This is the forty-fifth issue of a quarterly publication providing information on the technical work of the National Institute of Standards and Technology Electronics and Electrical Engineering Laboratory (EEEL). This issue of the EEEL Technical Progress Bulletin covers the fourth quarter of calendar year 1993.

Organization of Bulletin: This issue contains abstracts for all relevant papers released for publication by NIST in the quarter and citations and abstracts for such papers published in the quarter. Entries are arranged by technical topic as identified in the Table of Contents and alphabetically by first author under each subheading within each topic. Unpublished papers appear under the subheading "Released for Publication." This does not imply acceptance by any outside organization. Papers published in the quarter appear under the subheading "Recently Published." Following each abstract is the name and telephone number of the individual to contact for more information on the topic (usually the first author). This issue also includes a calendar of Laboratory conferences and workshops planned for calendar years 1994/1995 and a list of sponsors of the work.

Electronics and Electrical Engineering Laboratory: EEEL programs provide national reference standards, measurement methods, supporting theory and data, and traceability to national standards. The metrological products of these programs aid economic growth by promoting equity and efficiency in the marketplace, by removing metrological barriers to improved productivity and innovation, by increasing U.S. competitiveness in international markets through facilitation of compliance with international agreements, and by providing technical bases for the development of voluntary standards for domestic and international trade. These metrological products also aid in the development of rational regulatory policy and promote efficient functioning of technical programs of the Government.

The work of the Laboratory is conducted by four technical research Divisions: the Semiconductor Electronics and the Electricity Divisions in Gaithersburg, Md., and the Electromagnetic Fields and Electromagnetic Technology Divisions in Boulder, Colo. In 1991, the Office of Law Enforcement Standards, formerly the Law Enforcement Standards Laboratory, was transferred to EEEL. This Office conducts research and provides technical services to the U.S. Department of Justice and State and local governments, and other agencies in support of law enforcement activities. In addition, the Office of Microelectronics Programs (OMP) was established in EEEL to coordinate the growing number of semiconductor-related research activities at NIST. Reports of work funded through the OMP are included under the heading "Semiconductor Microelectronics."

Key contacts in the Laboratory are given on the inside back cover; readers are encouraged to contact any of these individuals for further information. To request a subscription or for more information on the Bulletin, write to EEEL Technical Progress Bulletin, National Institute of Standards and Technology, Metrology Building, Room B-358, Gaithersburg, MD 20899 or call (301) 975-2220.

Laboratory Sponsors: The Laboratory Programs are sponsored by the National Institute of Standards and Technology and a number of other organizations, in both the Federal and private sectors; these are identified on page 27.

Note on Publication Lists: Publication lists covering the work of each division are guides to earlier as well as recent work. These lists are revised and reissued on an approximately annual basis and are available from the originating division. The current set is identified in the Additional Information section, page 23.

Certain commercial equipment, instruments, or materials are identified in this paper in order to specify adequately the experimental procedures. Such identification does not imply recommendation or endorsement by the National Institute of Standards and Technology, nor does it imply that the materials or equipment identified are necessarily the best available for the purpose.

TABLE OF CONTENTS

FUNDAMENTAL ELECTRICAL MEASUREMENTS

Released for Publication

Early, E.A., and Clark, A.F., **The ac Josephson Effect in Parallel Junction Arrays.**

A general model of an arbitrary number of Josephson junctions in a parallel array is presented, in which the junctions are described by the resistively shunted junction model, and inductances, magnetic fields, and junction parameters are included. The differential equations which describe this model are derived. Current-voltage curves obtained from numerical solutions of these equations have, in addition to the usual integral Shapiro steps resulting from the ac Josephson effect, half-integral steps. Extensive simulations of the dependence of the step widths on ac current amplitude for two and three junctions in parallel show a variety of behaviors for both the integral and half-integral steps. Selected results are used in the companion paper, "Evidence for Parallel Junctions within High-T_c Grain-Boundary Junctions," to verify our proposal that half-integral steps in high-T_c grain-boundary junctions are a manifestation of a parallel array of junctions. Some results for the time dependence of various physical quantities are also presented.
[Contact: Alan F. Clark, (301) 975-2139]

Early, E.A., Steiner, R.L., Clark, A.F., and Char, K., **Evidence for Parallel Junctions within High-T_c Grain-Boundary Junctions.**

Novel half-integral constant voltage steps were observed in many high-T_c grain-boundary Josephson junctions of $YBa_2Cu_3O_{7-\delta}$ when a microwave field was applied. Five distinct observed behaviors of the widths of both integral and half-integral steps as a function of microwave amplitude, $\Delta I_{dc}(I_{ac})$, are reproduced by simulations of two or three junctions in parallel using the model presented in the companion paper, "The ac Josephson Effect in Parallel Junction Arrays." This provides quantitative evidence that a single high-T_c grain-boundary junction is composed of several junctions in parallel. These junctions are formed by the overlap of superconducting filaments on either side of the grain boundary. The spacing between junctions with large critical currents is $\sim 20\ \mu m$.
[Contact: Alan F. Clark, (301) 975-2139]

Lee, K.C., Cage, M.E., and Rowe, P.S., **Sources of Uncertainty in a DVM-Based Measurement System for a Quantized Hall Resistance Standard.**

Transportable 10-kΩ standard resistors have become fairly widespread in industrial, university, and government standards laboratories because of their low temperature coefficient of resistance, ease of transportation, and convenient value. The values of these resistors, however, tend to drift with time, requiring periodic recalibration against an absolute standard such as the quantized Hall resistance. The availability of a simple, inexpensive measurement system for calibrating 10-kΩ resistors against this absolute standard would be of great benefit to such primary standards laboratories. This paper describes a simple automated measurement system using a single, high-accuracy, commercially available digital voltmeter to compare the voltages developed across a 10-kΩ standard resistor and a quantized Hall resistor when the same current is passed through the two devices. From these measurements, the value of the 10-kΩ standard resistor is determined. The sources of uncertainty in this system are analyzed in detail, and it is shown that it is possible to perform calibrations with uncertainties in the range of 0.1 ppm.
[Contact: Kevin C. Lee, (301) 975-4236]

Martinis, J., Nahum, M., and Jensen, H.D., **Metrological Accuracy of the Electron Pump.**

We have operated a five-junction electron pump with an error for transferring electrons of approximately 0.5 ppm. The predicted error from previous theoretical considerations is expected to be several orders of magnitude smaller, thus implying that our present understanding of Coulomb blockade is incomplete. We conjecture that the errors arise from photon assisted tunneling, where the photon energy is supplied by noise from the environment.
[Contact: John M. Martinis, (303) 497-3597]

SEMICONDUCTOR MICROELECTRONICS

Silicon Materials

Released for Publication

Albers, J., **An Exact Solution of the Steady-State Surface Temperature for a General Multilayer Structure**, to be published in the Proceedings of the 1994 SEMI-THERM Conference, San Jose, California, February 1-3, 1994.

A recursion relation technique has been used in the past to determine the surface potential from the multilayer electrical Laplace equation. This has provided for a vastly simplified evaluation of the electrical spreading resistance and four-probe resistance. The isomorphism of the multilayer Laplace equation and the multilayer steady-state heat flow equation suggests the possibility of developing a recursion relation applicable to the multilayer thermal problem. This recursive technique is developed and is shown to provide the surface temperature of the multilayer steady-state heat flow equation. For the three-layer case, the thermal recursion relation readily yields the surface results which are identical with those presented by Kokkas and the TXYZ thermal code. This recursive technique can be used with any number of layers while incurring only a small increase in computation time for each added layer. For the case of complete, uniform top-surface coverage by a heat source, the technique gives rise to the generalized one-dimensional thermal resistance result. An example of the use of the new recursive method is provided by the preliminary calculations of the surface temperature of a buried oxide (SOI, SIMOX) structure containing several thicknesses of the surface silicon layers. This new technique should prove useful in the investigation and understanding of the steady-state thermal response of modern multilayer microelectronic structures.
[Contact: John Albers, (301) 975-2075]

Park, J.C., Lee, J.D., Venables, D., Krause, S.J., and Roitman, P., **Evolution of Dislocation Half-Loops into Defect Pairs during Thermal Processing of Oxygen-Implanted Silicon-On-Insulator Material**.

The effect of intermediate temperature annealing on defect evolution in contemporary oxygen-implanted silicon-on-insulator (SIMOX) material was investigated by transmission electron microscopy and defect etching. Extrinsic, prismatic dislocation half-loops on {110} planes at a density of $\sim 10^8$ cm^{-2} extended downward from the wafer surface during implantation. During annealing, ~1% of these half-loops expanded to the buried oxide, forming pairs of through-thickness defects. These defect pairs produce the etch-pit pairs commonly observed in defect etching studies. Thus, through-thickness defect pairs in contemporary SIMOX originate from dislocation half-loops in the as-implanted state. Possible half-loop formation mechanisms and their implications for defect density reduction are discussed.
[Contact: Peter Roitman, (301) 975-2077]

Silicon Materials

Recently Published

Korman, C.E., Mayergoyz, I.D., Gaitan, M., Tai, G-C., **An Efficient Method to Compute the Maximum Transient Drain Current Overshoot In Silicon On Insulator Devices**, Journal of Applied Physics, Vol. 73, No. 6, pp. 2611-2616 (March 15, 1993).

We present an efficient method to compute the maximum transient drain current overshoot in silicon-on-insulator metal-oxide silicon field effect transistors. The method is based on the physical idea that the number of majority carriers remains unchanged immediately after a change in the applied gate bias. The maximum overshot is computed by solving the Poisson and the stationary minority carrier transport equations under the constraint that the number of majority carriers is conserved. Hence, the novel aspect of the method is that it allows one to compute the maximum drain current overshoot without resorting to a computationally costly transient simulation. The accuracy of the method is verified by comparing the value of the drain current computed by this method with the maximum value of the drain current computed by transient simulations. The comparisons show that, with this method, the maximum transient drain current overshoot can be computed quite accurately for fast changes in the gate bias.
[Contact: Michael Gaitan, (301) 975-2070]

Compound Materials

Released for Publication

Albers, J., **An Exact Solution of the Steady-State Surface Temperature for a General Multilayer Structure**, to be published in the Proceedings of the 1994 SEMI-THERM Conference, San Jose, California, February 1-3, 1994.

[See Silicon Materials.]

Lowney, J.R., Wang, L., and Haegel, N.M., **Band-to-Band Photoluminescence and Luminescence Excitation in Extremely Heavily Carbon-Doped Epitaxial GaAs**.

Heavily carbon-doped GaAs samples with doping levels as high as 4.1 x 10^{20} cm^{-3} were studied by photoluminescence and luminescence excitation spectroscopies. Luminescence and absorption bandgaps were determined, from which the positions of the observed emission spectra, including diffraction and refraction of the luminescence, substrate effects, and lattice contraction in the carbon-doped epilayer, were examined. A first-principles calculation was performed to calculate the density of states, bandgap, Fermi energy, and emission spectrum. Comparison of calculation results with the experiments shows that the theoretical model we use is a good approximation for describing band structure for doping levels higher than 10^{20} cm^{-3}. However, the discrepancy between the measured and the calculated emission spectra indicates that the usual assumptions such as constant momentum matrix elements and quasi-equilibrium distribution of photo-excited electrons in the conduction band may not be appropriate in treating the transition processes in highly degenerate semiconductors.
[Contact: Jeremiah R. Lowney, (301) 975-2048]

Lowney, J.R., Kim, J.S., and Seiler, D.G., **Magnetotransport Properties of HgCdTe**.

Magnetotransport techniques are widely used to characterize the electrical properties of HgCdTe. The Hall-effect method is the most common method of determining the carrier density and mobility of semiconductor materials. Multicarrier characterization techniques are needed for determination of carrier densities and mobilities in a multicarrier system present in layered structures or in a variety of complex semiconductor materials. Because of the importance of these methods for proper electrical characterization of complex HgCdTe single crystals or layered-structures, we discuss this topic pedagogically with the primary objective of promulgation of this emerging tool to the HgCdTe characterization community. We also discuss magnetoresistance and magnetoresistance-based techniques such as the Shubnikov-de Haas effect and magnetophonon effect, which have been used to characterize HgCdTe materials. These techniques are all capable of providing very accurate data if applied with care and proper analysis.
[Contact: Jeremiah R. Lowney, (301) 975-2048]

McCallum, D.S., Cartwright, A.N., Smirl, A.L., Tseng, W.F., Pellegrino, J.G., and Comas, J., **Enhancement of the Per-Carrier Nonlinear Cross Sections in GaAs/AlGaAs Hetero n-i-p-i's**.

An enhancement of the change in absorption coefficient per electron-hole pair, σ_{ch}, is observed as the number of quantum wells in each intrinsic region is increased in otherwise identical hetero n-i-p-i's. This enhancement is directly proportional to the number of quantum wells per intrinsic region, but is accompanied by a simultaneous reduction in the saturation carrier density for the nonlinearity that is inversely proportional to the number of quantum wells per intrinsic region. Taken together, these results demonstrate that, by controlling the number of wells per intrinsic region, dynamic range can be traded for sensitivity in device applications.
[Contact: Wen F. Tseng, (301) 975-5291]

Tobin, S.P., Tower, J.P., Norton, P.W., Chandler-Horowitz, D., Amirtharaj, P.M., Lopes, V.C., Duncan, W.M., Syllaios, A.J., Ard, C.K., Giles, N.C., Balasubramanian, R., Bollong, A.B., Steiner, T.W., Bowen, D.K., and Tanner, B.K., **A Comparison of Techniques for Nondestructive Composition Measurements in $Cd_{1-x}Zn_xTe$ Substrates**, to be published in the 1993 U.S. Workshop on the Physics and Chemistry of Mercury Cadmium Telluride and Other IR Materials, Seattle, Washington, October 19-21, 1993.

We report an overview and comparison of nondestructive optical techniques for determining alloy composition x in $Cd_{1-x}Zn_xTe$ substrates for HgCdTe epitaxy. The methods for single-point measurements include a new x-ray diffraction technique for precision lattice parameter measurements using a standard high-resolution diffractometer, room-temperature photoreflectance, and low-temperature photoluminescence. We compare measurements on the same set of samples by all three techniques. Comparisons of precision and accuracy, with a discussion of the strengths and weaknesses of different techniques, are presented. In addition, a new photoluminescence excitation technique for full-wafer imaging of composition variations is described.
[Contact: Deane Chander-Horowitz, (301) 975-2084]

Compound Materials

Recently Published

Friedman, D.J., Zhu, J.G., Kibbler, A.E., Olson, J.M., and Moreland, J., **Surface Topography and Ordering-Variant Segregation in $GaInP_2$**, Applied Physics Letters, Vol. 63, No. 13, pp. 1774-1776 (September 27, 1993).

Using transmission electron diffraction dark-field imaging, atomic force microscopy (AFM), and Nomarski microscopy, we demonstrate a direct connection between surface topography and cation site ordering in $GaInP_2$. We study epilayers grown by organometallic vapor-phase epitaxy on GaAs substrates oriented 2° off (100) towards (110). Normarski microscopy shows that, as growth proceeds, the surface of ordered material forms faceted structures aligned roughly along [011]. A comparison with the dark-field demonstrates that the $[1\bar{1}1]$ and $[11\bar{1}]$ ordering variants are segregated into complementary regions corresponding to opposite-facing facets of the surface structures. This observation cannot be rationalized with the obvious but naive model of the surface topography as being due to faceting into low-index planes. However, AFM reveals that the facets are, in fact, *not* low-index planes, but rather are tilted 4° from (100) towards $(111)_B$. This observation explains the segregation of the variants: the surface facets act as local $(111)_B$- misoriented growth surfaces which select only one of the two variants.
[Contact: John Moreland, (303) 497-3641]

Lowney, J.R., Seiler, D.G., Thurber, W.R., Yu, Z., Song, X.N., and Littler, C.L., **Heavily Accumulated Surfaces of Mercury Cadmium Telluride Detectors: Theory and Experiment**, Journal of Electronic Materials, Vol. 22, No. 8, pp. 985-991, January 4, 1993.

Some processes used to passivate *n*-type mercury-cadmium-telluride photoconductive infrared detectors produce accumulation layers at the surfaces which result in 2D electron gases. The dispersion relations for the electric subbands that occur in these layers have been calculated from first principles. Poisson's equation for the built-in potential and Schroedinger's equation for the eigenstates have been solved self-consistently. The cyclotron effective masses and Fermi energies have been computed for each subband density for 12 total densities between 0.1 to 5.0×10^{12} cm^{-2}. The agreement with Shubnikov-de Haas measurements is very good at lower densities with possible improvement if band-gap narrowing effects were to be included. At higher densities larger differences occur. The simple 2D description is shown to break down as the density increases because the wave functions of the conduction and valence bands cannot be well separated by the narrow band gap of long-wavelength detectors. These results provide a basis for characterizing the passivation processes, which greatly affect device performance.
[Contact: Jeremiah R. Lowney, (301) 975-2048]

Device Physics and Modeling

Recently Published

Lowney, J.R., Seiler, D.G., Thurber, W.R., Yu, Z., Song, X.N., and Littler, C.L., **Heavily Accumulated Surfaces of Mercury Cadmium Telluride Detectors: Theory and Experiment**, Journal of Electronic Materials, Vol. 22, No. 8, pp. 985-991, January 4, 1993.

[See Compound Materials.]

Insulators and Interfaces

Released for Publication

Albers, J., **An Exact Solution of the Steady-State Surface Temperature for a General Multilayer Structure**, to be published in the Proceedings of the 1994 SEMI-THERM Conference, San Jose, California, February 1-3, 1994.

[See Silicon Materials.]

Chandler-Horowitz, D., Pellegrino, J.G., Nguyen, N.V., Amirtharaj, P.M., and Qadri, S.B., **Interface Roughness Induced Changes in the Near-E_0 Spectroscopic Behavior of Short-Period GaAs/AlAs Superlattices**, to be published in the Proceedings of the Materials Research Society, Boston, Massachusetts, November 29, 1993—December 3, 1993.

The perturbations introduced by the increasing degree of interface roughness on the optical properties of 3 x 3 short-period GaAs/AlAs superlattices (SL) were investigated through an examination of the position and line shape of the E_0 (direct gap) feature in photoreflectance and spectroscopic ellipsometry. The measured spectra were compared to that from an $Al_xGa_{1-x}As$ ($x \approx 0.5$) alloy reference specimen grown under near identical conditions. The degree of interface roughness in the SLs was controlled by a choice of the growth conditions and the buffer layer thickness. The structural behavior was characterized by X-ray diffraction. The results show that the increasing interface roughness enlarges the linewidth, Γ, from 42 meV to 64 meV, and the corresponding transition energy, E_0, shifts from 2.060 eV to 2.112 eV; the reference values from the $Al_xGa_{1-x}As$ ($x \approx 0.5$) sample are 25 meV and 2.136 eV, respectively. The upshift of E_0 from the SLs with increasing interface roughness may be understood as a consequence of the roughening-induced intermixing and the eventual reduction in the modulation depth of the SL potential. The increase of Γ also with roughening suggests that additional mechanisms, such as roughening-induced scattering are important. The Γ and E_0 values from an $Al_{0.5}Ga_{0.5}As$ alloy sample are valuable in this comparative analysis since they represent the lowest and highest bounds for the SL Γ and E_0, respectively.

[Contact: Deane Chandler-Horowitz, (301) 975-2084]

Nguyen, N.V., Chandler-Horowitz, D., Amirtharaj, P.M., and Pellegrino, J.G., **Spectroscopic Ellipsometry Determination of the Properties of the Thin Underlying Strained Si Layer and the Roughness at SiO_2/Si Interface**.

The strain at the interface of thermally grown SiO_2 films on Si was determined for the first time by high-accuracy spectroscopic ellipsometry. The dielectric function of the interface was unambiguously determined by a comprehensive data analysis procedure. By carefully examining the dielectric function, we quantitatively determined the thickness of both the underlying strained silicon to be about 1.5 nm and the interfacial roughness to be about 0.7 nm. The strain was seen to cause a redshift of 0.04 eV of the interband critical point E_1 compared with the bulk silicon value.
[Contact: Nhan V. Nguyen, (301) 975-2044]

Dimensional Metrology

Released for Publication

Marchiando, J.F., **On Calculating the Reflectance and Transmittance of Light for a Simple Thick Grating Structure**.

This paper presents a formulation for calculating the reflectance and transmittance of classical light for a simple structure that contains a rectangularly shaped line grating layer that lies atop a thick transparent or weakly absorbing substrate layer. It is assumed that the substrate thickness is sufficiently large and/or nonuniform that light tranversing it loses phase coherence and intensities can be added. It is also assumed that the optical properties of the media in the various homogeneous regions of the structure are complex, local, linear, isotropic, and nonmagnetic. This kind of structure has important applications in the metrology of linewidths for the semiconductor integrated circuit industry.
[Contact: Jay F. Marchiando, (301) 975-2088]

Dimensional Metrology

Recently Published

Allen, R.A., Troccolo, P., Owen III, J.C., Potzick, J.E., and Linholm, L.W., **Comparisons of Measured Linewidths of Sub-Micrometer Lines Using Optical, Electrical, and SEM Metrologies**, Proceedings of SPIE (The International Society for Optical Engineering, P.O. Box 10, Bellingham, Washington 98227-0010), Integrated Circuit Metrology, Inspection, and Process Control VII, Vol. 1926, pp. 34-43 (1993).

An investigation was carried out to determine the ability of three methods of linewidth metrology to measure the dimensions of features to less than 0.5 μm. The three methods are transmitted-light optical microscopy, electrical test structure, and scanning electron microscopy (SEM). Electrical, SEM, and reflected-light microscopy techniques are widely used for linewidth metrology in VLSI fabrication. However, none of these widely-used techniques currently permits traceability to international standards of length. Transmitted-light optical microscopy allows traceability; however, this technique is applicable only to transparent substrates. To permit the inclusion of transmitted-light optical microscopy in this investigation, 100-nm thick Ti films were patterned using normal VLSI processing techniques on a 150-mm diameter quartz wafer. The cross-bridge resistor test structure was used since this structure has been widely used in industry, and it allows the results from all three metrological techniques to be compared. The design bridge widths of the test structures range from 0.4 μm to 1.0 μm. The results of these measurements show systematic and uniform offsets between the different techniques. In this paper, we discuss the different techniques and describe the observed results.
[Contact: Richard A. Allen, (301) 975-5026]

Postek, M.T., Lowney, J.R., Vladar, A.E., Keery, W.J., Marx, E., and Larrabee, R.D., **X-Ray Lithography Mask Metrology: Use of Transmitted Electrons in an SEM for Linewidth Measurement**, Journal of Research of the National Institute of Standards and Technology, Vol. 98, No. 4, pp. 415-445 (July/August 1993).

X-ray masks present a measurement object that is different from most other objects used in semiconductor processing because the support membrane is, by design, X-ray transparent. This characteristic can be used as an advantage in electron beam-based X-ray mask metrology since, depending upon the incident electron beam energies, substrate composition and substrate thickness, the membrane can also be essentially electron transparent. The areas of the mask where the absorber structures are located are essentially X-ray opaque, as well as electron opaque. This paper shows that excellent contrast and signal-to-noise levels can be obtained using the transmitted-electron signal for mask metrology rather than the more commonly collected secondary electron signal. Monte Carlo modeling of the transmitted electron signal was used to support this work in order to determine the optimum detector position and characteristics, as well as in determining the location of the edge in the image profile. The comparison between the data from the theoretically modeled electron-beam interaction and actual experimental data was shown to agree extremely well, particularly with regard to the wall slope characteristics of the structure. Therefore, the theory can be used to identify the location of the edge of the absorber line for linewidth measurement. This work provides one approach to improved X-ray masks in commercial instrumentation. This work also represents an initial step toward the first scanning electron microscope-based accurate linewidth measurement standard from NIST, as well as providing a viable metrology for linewidth measurement instruments of X-ray masks for the lithography community.
[Contact: Michael T. Postek, (301) 975-2299]

Integrated-Circuit Test Structures

Released for Publication

Linholm, L.W., Allen, R.A., and Cresswell, M.W., **Microelectronic Test Structures for Feature Placement and Electrical Linewidth Metrology**, to be published in the Proceedings of SPIE (The International Society for Optical Engineering, P.O. Box 10, Bellingham, Washington 98227-0010), Microelectronic Processing '93 Symposium, Monterey, California, September 27-29, 1993.

Control of feature placement and control of linewidth have been and are expected to continue to be two of the most important challenges required in the manufacturing of advanced microelectronic devices.

By the year 2001, it is anticipated that typical linewidth resolution of 180 nm must be imaged over an approximate 1000-mm^2 image field with level-to-level overlay requirements on the order of 60 nm. Lithographic tools capable of such placement are being developed. Accurate and precise determination of linewidth and feature placement become dimensions of devices important for process characterization and control as the design dimensions of devices decrease. Traditional methods of measuring these parameters suffer from both measurement speed and equipment expense. In addition, making precise measurements of features below 0.5 μm is becoming very difficult due to the difficulty in determining the physical location of the edge. Microelectronic test structures provide low-cost, post-patterning metrology for determining both feature placement and electrical linewidth. They are supported by a variety of commercial test equipment often found in semiconductor manufacturing facilities. Properly characterized test structures and measurement methods provide an economic means of determining the critical parameters needed to develop, control, and operate the next generation of patterning tools. This paper presents a review of test structures and test methods used for determining feature placement and electrical linewidth.
[Contact: Loren W. Linholm, (301) 975-2052]

Marshall, J.C., and Zaghloul, M.E., ***Semiconductor Measurement Technology*: Design and Testing Guides for the CMOS and Lateral Bipolar-On-SOI Test Library**, to be published as NIST Special Publication 400-93.

Design and testing guides have been developed for the test library from which test chip NIST8 and test wafer NIST9 were derived. They were designed for use in process monitoring and device parameter extraction to evaluate and compare CMOS (Complementary Metal-Oxide-Semiconductor) test structures, including devices and circuits, fabricated on both bulk silicon and SOI (Silicon-on-Insulator), specifically SIMOX (Separation by the IMplantation of OXygen), wafers. The test library consists of both CMOS-on-SOI and lateral bipolar-on-SOI modules. From it, 20 modules were assembled to create CMOS test chip NIST8 that was fabricated using a standard bulk CMOS foundry through the MOSIS service. SOI/SIMOX test wafer NIST9 contains approximately 1000 modules and was also assembled from modules in this test library. Fourteen processing masks are used to fabricate depletion-mode MOSFETs, lateral bipolar devices, and CMOS MOSFETs with source-to-channel ties. The SOI/SIMOX technology file used with the Magic VLSI layout editor was modified to include the layers necessary to generate these 14 processing masks. This modification is discussed, and unique test structure designs are presented.
[Contact: Janet C. Marshall, (301) 975-2049]

Marshall, J.C., and Zaghloul, M., **Color Supplement to NIST Special Publication 400-93: CMOS and Lateral Bipolar-On-SOI Test Structures**, to be published as NISTIR 5324.

This report is the supplement to the NIST Special Publication entitled, "*Semiconductor Measurement Technology:* Design and Testing Guides for the CMOS and Lateral Bipolar-on-SOI Test Library." This supplement contains the complete set of figures from the above mentioned document with the test structures provided in color for easier interpretation.
[Contact: Janet C. Marshall, (301) 975-2049]

Integrated-Circuit Test Structures

Recently Published

Allen, R.A., and Schuster, C.E., **An Electrical Test Structure for Improved Measurement of Feature Placement and Overlay in Integrated Circuit Fabrication Processes**, Proceedings of the Government Microcircuit Applications Conference 1993, New Orleans, Louisiana, November 1-5, 1993, pp. 159-161.

The modified voltage-dividing potentiometer has previously been demonstrated to have a resolution of under 10 nm when applied to short-loop, single-level processes. This test structure has recently been applied to several full cycle processes, which we are reporting here for the first time. In this paper, we describe the successful demonstration of test vehicle implementations and test results obtained from applying the new design to a GaAs Microwave/Millimeter Wave Monolithic Integrated Circuits process and a CMOS/Bulk process. The

demonstrated success in these substantially different processes indicates that these results should apply to a wide range of semiconductor fabrication environments.
[Contact: Richard A. Allen, (301) 975-5026]

Microfabrication Technology

Released for Publication

Hebner, R.E., **Directions in Microelectromechanical Systems Research Application Development**, to be published in the Proceedings of the Microsensor and Micromachines Conference, Alexandria, Virginia, December 6-7, 1993.

NIST's laboratory-based metrology programs are planned and implemented in cooperation with industry and focus on measurements, standards, evaluated data, and test methods. It is as part of this program that NIST is developing microelectromechanical systems (MEMS). The NIST program has three primary thrusts: the development of MEMS-based devices for metrology applications; materials characterization, and standards.
[Contact: Robert E. Hebner, (301) 975-2220]

Plasma Processing

Recently Published

Olthoff, J.K., **Gaseous Electronics Conference RF Reference Cell Newsletter**, Vol. 5, No. 1, pp. 1-2 (May 1993).

This newsletter provides users of Gaseous Electronics Conference (GEC) rf Reference Cells with information on related research projects. This issue summarizes the research projects using GEC cells at 10 different laboratories and provides the first list of GEC-cell-related publications.
[Contact: James K. Olthoff, (301) 975-2431]

Packaging

Recently Published

Carpenter, J.A., Jr., Dickens, B., Kreider, K.G., Manning, J.R., Mattis, R.L., Piermarini, G.J., Read, D.T., and Evans, R.D., **NIST/NCMS Program on Electronic Packaging: First Update**, Ceramic Transactions, Materials in Microelectronic and Optoelectronic Packaging, Vol. 33, pp. 345-358 (1993).

In 1992, the National Institute of Standards and Technology expanded its intermural efforts on development of metrology for microelectronics packaging and interconnection. The new intramural projects concentrate on development or refinement of metrology for measuring the properties of the materials as they actually exist in modern packaging and interconnection, and not as measured on idealized or bulk specimens. The metrology is intended for use in research, manufacturing, product quality control and failure analysis. Also, work begun in 1991 accelerated in a major consortium effort led by The National Center for Manufacturing Sciences and jointly supported by the consortium members and the NIST Advanced Technology Program to develop new materials and production technology for printed wiring boards. This is an update on the progress of those efforts.
[Contact: Richard L. Mattis, (301) 975-2235]

Photodetectors

Released for Publication

Lowney, J.R., Kim, J.S., and Seiler, D.G., **Magnetotransport Properties of HgCdTe**.

[See Compound Materials.]

Photodetectors

Recently Published

Hale, P.D., and Franzen, D.L., **Accurate Characterization of High Speed Photodetectors**, Proceedings of SPIE (The International Society for Optical Engineering, P.O. Box 10, Bellingham, Washington 98227-0010), Photodetectors and Power Meters, Vol. 2022, pp. 218-227 (1993).

We designed a simple heterodyne system for frequency domain photodetector characterization which is intended to avoid many of the disadvantages of earlier characterization systems and to minimize errors due to intensity fluctuation, frequency calibration, and source impedance

mismatch without using vector network analysis. A detailed uncertainty analysis for the system indicates 95% confidence intervals between ±0.25 and ±0.6 dB at 25 GHz, depending on the photodetector output impedance.
[Contact: Paul D. Hale, (303) 497-5367]

Lowney, J.R., Seiler, D.G., Thurber, W.R., Yu, Z., Song, X.N., and Littler, C.L., **Heavily Accumulated Surfaces of Mercury Cadmium Telluride Detectors: Theory and Experiment**, Journal of Electronic Materials, Vol. 22, No. 8, pp. 985-991, January 4, 1993.

Some processes used to passivate *n*-type mercury-cadmium-telluride photoconductive infrared detectors produce accumulation layers at the surfaces which result in 2D electron gases. The dispersion relations for the electric subbands that occur in these layers have been calculated from first principles. Poisson's equation for the built-in potential and Schroedinger's equation for the eigenstates have been solved self-consistently. The cyclotron effective masses and Fermi energies have been computed for each subband density for 12 total densities between 0.1 to 5.0 × 10^{12} cm^{-2}. The agreement with Shubnikov-de Haas measurements is very good at lower densities with possible improvement if band-gap narrowing effects were to be included. At higher densities larger differences occur. The simple 2D description is shown to break down as the density increases because the wave functions of the conduction and valence bands cannot be well separated by the narrow band gap of long-wavelength detectors. These results provide a basis for characterizing the passivation processes, which greatly affect device performance.
[Contact: Jeremiah R. Lowney, (301) 975-2048]

Other Semiconductor Metrology Topics

Released for Publication

Scace, R.I., **Measurements - What Next?**

Semiconductor manufacturing is evolving from being an empirical art into an industry based increasingly on physical understanding and real-time process control. Both understanding and control require correctly applied measurement tools, many of which do not now exist in suitable form. In addition, the continuing drive toward smaller geometries and more complex chips leads directly to demands on metrology that cannot be met using refinements of today's technology. New approaches to measurement will often be necessary.
[Contact: Robert I. Scace, (301) 975-4400]

SIGNAL ACQUISITION, PROCESSING, AND TRANSMISSION

DC and Low-Frequency Metrology

Recently Published

Avramov, S., and Oldham, N.M., **Automatic Calibration of Inductive Voltage Dividers for the NASA Zeno Experiment**, Review of Scientific Instruments, Vol. 64, No. 9, pp. 2676-2678 (September 1993).

Two inductive voltage dividers (IVDs) used for temperature measurements in NASA's zeno experiment were tested. In order to obtain the required resolution of 10 parts-per-billion, a 30-bit binary inductive voltage divider developed at the National Institute of Standards and Technology was used to measure the differential linearity of the Zeno IVDs. Automatic measurements were performed on the dividers in the Zeno experiment engineering model at frequencies of 266 Hz and 351 Hz over a ratio range of 0.55 to 0.56. The measured differential linearity limits the temperature resolution to 5 μK.
[Contact: Nile M. Oldham, (301) 975-2408]

Cryoelectronic Metrology

Released for Publication

Berkowitz, S.J., Skocpol, W.J., Mankiewich, P.M., Ono, R.H., Missert, N.A., Rosenthal, P.A., and Vale, L.R., **Thermal Noise in High Temperature Superconducting-Normal-Superconducting Step-Edge Josephson Junctions**.

We have fabricated $YBa_2Cu_3O_{7-\delta}$-Ag-$YBa_2Cu_3O_{7-\delta}$ step-edge Josephson junctions that fit the resistively shunted junction (RSJ) model with Johnson-Nyquist thermal noise. The I-V curves are well fit over a large temperature range for junctions of varying critical current values. There is good agreement

between the fitted thermal noise temperature and the measured ambient temperature. This is strong evidence that these junctions are not dominated by superconducting shorts longer than the superconducting coherence length. In addition, no excess current is observed in these junctions, which is expected in a perfect RSJ junction.
[Contact: Ronald H. Ono, (303) 497-3762]

Early, E.A., and Clark, A.F., **The ac Josephson Effect in Parallel Junction Arrays**.

[See Fundamental Electrical Measurements.]

Early, E.A., Clark, A.F., and Lobb, C.J., **Physical Basis For Half-Integral Shapiro Steps In a dc SQUID**.

The dynamics of a dc superconducting quantum interference device (SQUID) is analogous to the classical dynamics of a particle subject to conservative, damping, and driving forces in two dimensions. The equations of motion define a trajectory on a potential energy surface derived from the conservative forces, the components of which correspond to different forms of stored energy in the SQUID. In the presence of a periodic driving force, half-integral Shapiro steps are possible when the trajectory follows a zig-zag path between minima of the potential surface. This description of the dynamics in terms of a potential surface provides an intuitive, physical basis for previous simulation results on half-integral Shapiro steps in a dc SQUID.
[Contact: Alan F. Clark, (301) 975-2139]

Early, E.A., Steiner, R.L., Clark, A.F., and Char, K., **Evidence for Parallel Junctions within High-T_c Grain-Boundary Junctions**.

[See Fundamental Electrical Measurements.]

Ludwig, F., Dantsker, E., Nemeth, D.T., Koelle, D., Miklich, A.H., Clarke, J., Knappe, S., Koch, H., and Thomson, R.E., **Fabrication Issues in Optimizing $YBa_2Cu_3O_{7-\delta}$ Flux Transformers for Low l/f Noise**.

We describe an improved interconnect technology for the fabrication of multiturn flux transformers from $YBa_2Cu_3O_{7-\delta}$-$SrTiO_3$-$YBa_2Cu_3O_{7-\delta}$ multilayers. The essential improvements are reductions in the thickness of the trilayer films, typically to 100 nm, and 250 nm, respectively, and in the deposition rate, to 0.07 nm/laser pulse. This process yields crossovers in which the critical current density in the upper film at 77 K is (2 to 3) x 10^6 A cm^{-2}. *In-situ* trilayers exhibited l/f flux noise levels at 1 Hz below the measurement sensitivity of 10 $m\Phi_0$ $Hz^{-1/2}$, where Φ_0 is the flux quantum. However, the flux noise of trilayers in which each layer had been patterned was significantly higher. The best flip-chip magnetometer had a white noise of 40 fT $Hz^{-1/2}$, increasing to 340 fT $Hz^{-1/2}$ at 1 Hz; the corresponding flux noise levels were 9 $m\Phi_0$ $Hz^{-1/2}$ and 75 $m\Phi_0$ $Hz^{-1/2}$, respectively.
[Contact: Robert E. Thomson, (303) 497-3141]

Reintsema, C.D., Ono, R.H., Harvey, T.E., Missert, N., and Vale, L.R., **Phase Locking in Two-Junction Systems of High-T_c Step-Edge S-N-S Junctions**.

Mutual phase locking between two high-critical-temperature step-edge superconducting-normal metal-superconducting junctions has been investigated. Using a two-junction circuit with an ex situ-deposited feedback resistor, the strength of the phase-locked state has been characterized as a function of locking frequency and temperature. Results are presented for a planar circuit as well as a multilayer circuit incorporating a superconducting ground plane. The observed behavior was significantly enhanced for the circuit over a ground plane. Characterization of the phase-locked state at 4 K yielded locking strengths as large as $|I_L|1\text{-}I_c$ = 9%, and maximum locking frequencies to l.06 THz. The magnitude of the locking strength was found to decrease rapidly with increasing temperature with complete loss of coherence occurring at temperatures greater than 35 K.
[Contact: Ronald H. Ono, (303) 497-3762]

Russek, S.E., Sanders, S.C., Roshko, A., and Ekin, J.W., **Surface Degradation of Superconducting $YBa_2Cu_3O_{7-\delta}$ Thin Films**.

The surface degradation of $YBa_2Cu_3O_{7-\delta}$ thin films due to air, CO_2, N_2, O_2, and vacuum exposure has been studied with reflection high-energy electron diffraction (RHEED), scanning tunneling microscopy, and contact resistivity measurements. The

formation of an amorphous surface reaction layer upon exposure to air and CO_2 is monitored with RHEED and correlated with an increase in contact resistivity. The contact resistivity, for air exposed samples, was found to increase with time t as $\rho_c = (1.2 \times 10^{-7} \Omega \cdot cm^2 \exp(\sqrt{t}/21 \text{ mm})$. CO_2-exposed surfaces showed a similar degradation, while N_2 exposed surfaces showed a different degradation mechanism. Vacuum-exposed surfaces show little increase in contact resistivity, indicating no long-term surface oxygen loss.
[Contact: Steven E. Russek, (303) 497-5097]

Wu, H., Galt, D., Price, J., and Beall, J.A., **Extracting the Dielectric Properties of Thin-Film $SrTiO_3$ Grown on $LaAlO_3$ Using $YBa_2Cu_3O_{7-x}$**, to be published in the Proceedings of SPIE (The International Society for Optical Engineering, P.O. Box 10, Bellingham, Washington 98227-0010), High T_c Microwave Superconductors and Applications Symposium, Los Angeles, California, January 24-28, 1994.

We have fabricated and characterized YBCO ($YBa_2Cu_3O_{7-x}$) microstrip resonators on LAO ($LaAlO_3$) substrates that include thin-film STO ($SrTiO_3$) coplanar capacitors to study the dielectric properties of thin-film STO. We measure the low-frequency capacitance of the STO/LAO capacitor as a function of temperature and dc bias. We use the observed resonant frequencies to extract the microwave frequency capacitance of the structure and the Qs to determine the microwave losses. We develop a conformal map and use it to transform the observed capacitances into dielectric constant values for the thin-film STO.
[Contact: James A. Beall, (303) 497-5989]

Cryoelectronic Metrology

Recently Published

Booi, P.A., Livingston, C.A., and Benz, S.P., **Intrinsic Stress in dc Sputtered Niobium**, IEEE Transactions on Applied Superconductivity, Vol. 3, No. 2, pp. 3029-3031 (June 1993).

The intrinsic mechanical stress of dc magnetron-sputtered Nb films is characterized as a function of sputtering parameters and target erosion. The zero-stress point shifts to lower cathode voltages as the target erodes. The zero-stress point was always characterized by the same cathode current-Ar pressure relationship.
[Contact: Peter A. Booi, (303) 497-5910]

Ekin, J.W., **Preparation of Low Resistivity Contacts for High-T_c Superconductors**, in Processing and Properties of High-T_c Superconductors, Vol. 1, Chapter 9 (World Scientific Publishing Company, Singapore, 1993), pp. 371-407.

Methods for preparing practical contacts to high-T_c superconductors are described, including quick, easy techniques for attachment of voltage-taps, and detailed descriptions of how to fabricate high-quality contacts for current connections. Methods for soldering and lead attachment that preserve the low resistivity of high-quality contacts are also presented.
[Contact: John W. Ekin, (303) 497-5448]

Moreland, J., **Tunneling Spectroscopy of Thallium-Based High Temperature Superconductors**, Chapter in Thallium-Based High-Temperature Superconductors, A.M. Hermann and J.V. Yakhmi, Eds. (Marcel Dekker, Inc., New York, NY, 1994), pp. 569-577.

This chapter focuses on electron tunneling spectroscopy of the thallium-based high-temperature superconductor materials. A summary of published results is included with comments regarding interpretations of each measurement. Other phenomena that may have subsequent bearing on the interpretation of tunneling spectra are addressed briefly including a linear background conductance, Coulomb blockage effects, and bound states at superconductor/normal metal interfaces. This chapter does not address many of the Josephson-like devices based on weak-links, point contacts, microbridges, or step-edge junctions.
[Contact: John Moreland, (303) 497-3641]

Peterson, R.L., **An Analysis of the Impact on U.S. Industry of the NIST/Boulder Superconductivity Programs: An Interim Study**, NISTIR 5012 (November 1993).

This report is an interim study of the impact of the NIST/Boulder superconductivity programs on U.S.

industry. Because the superconductor market is still small - the promising new technology of high-temperature superconductivity has not had time to significantly enter the marketplace - a detailed economic study of the NIST impact is not warranted. Nevertheless, it was felt useful to undertake a preliminary analysis of the impact of the NIST/Boulder programs. In this report, numerical estimates are made of the return on investment for areas which could be quantified. Anecdotal material and consideration of unquantified impacts are also included, and a survey of the U.S. superconductor industry is made. [Contact: Robert L. Peterson, (303) 497-3750]

Microwave and Millimeter-Wave Metrology

Released for Publication

Hill, D.A., Cavcey, K.H., and Johnk, R., **Crosstalk Between Microstrip Transmission Lines**.

Methods for prediction of crosstalk between microstrip transmission lines are reviewed and simplified for the weak coupling case. Classical coupled transmission line theory is used for uniform lines, and potential and induced electromagnetic field methods are used for crosstalk between nonuniform lines. It is shown that the potential method is equivalent to classical coupled transmission line theory for the case of uniform lines. An experiment was performed for uniform coupled microstrip lines for frequencies from 40 MHz to 5 GHz, and good agreement between theory and measurement was obtained for both near-end and far-end crosstalk.
[Contact: David A. Hill, (303) 497-3472]

Marks, R.B., and Williams, D.F., **Verification of Commercial Probe-Tip Calibrations**, to be published in the Conference Digest of the 42nd Automatic Radio Frequency Techniques Group (ARFTG), San Jose, California, December 2-3, 1993.

We present results of a verification procedure useful in evaluating the accuracy of probe-tip scattering parameter measurements. The procedure was applied to calibrations and measurements performed in industrial laboratories. Actual measurement discrepancies, due primarily to calibration errors, are directly compared to bounds determined by the comparison method. The results demonstrate the utility of the verification technique as well as serious flaws, particularly at high frequencies, in some conventional calibrations.
[Contact: Roger B. Marks, (303) 497-3037]

Williams, D.F., and Marks, R.B., **LRM Probe-Tip Calibrations with Imperfect Resistors and Lossy Lines**, to be published in the Conference Digest of the 42nd Automatic Radio Frequency Techniques Group (ARFTG), San Jose, California, December 2-3, 1993.

The Line-Reflect-Match (LRM) calibration is extended, without significant loss of measurement accuracy to accommodate imperfect match standards and lossy lines typical of monolithic microwave integrated circuits. We characterize the match and line standards using an additional line standard of moderate length. The new method provides a practical means of obtaining accurate, wideband calibrations with compact standard sets.
[Contact: Dylan F. Williams, (303) 497-3138]

Electromagnetic Properties

Released for Publication

Geyer, R.G., Krupka, J., Kuhn, M., and Hinken, J., **Dielectric Properties of Single Crystals of Al_2O_3, $LaAlO_3$, $NdGaO_3$, $SrTiO_3$, and MgO at Cryogenic Temperatures**.

A dielectric resonator technique has been used for measurements of the permittivity and dielectric loss tangent of single-crystal dielectrics in the temperature range 20 to 300 K at microwave frequencies. Application of superconducting films made it possible to determine dielectric loss tangents of about 5×10^{-7} at 20 K. Two permittivity tensor components for uniaxially anisotropic samples were measured. Generally, single-crystal samples made of the same material by different manufacturers or by different processes have significantly different losses, although they have essentially the same permittivities. The permittivity of one crystalline ferroelectric substrate, $SrTiO_3$, strongly depends on temperature. This temperature dependence can affect the performance of ferroelectric thin-film microwave devices, such as

electronically tunable phase shifters, mixers, delay lines, and filters.
[Contact: Richard G. Geyer, (303) 497-5852]

Wu, H., Galt, D., Price, J., and Beall, J.A., **Extracting the Dielectric Properties of Thin-Film $SrTiO_3$ Grown on $LaAlO_3$ Using $YBa_2Cu_3O_{7-x}$**, to be published in the Proceedings of SPIE (The International Society for Optical Engineering, P.O. Box 10, Bellingham, Washington 98227-0010), High T_c Microwave Superconductors and Applications Symposium, Los Angeles, California, January 24-28, 1994.

[See Cryoelectronic Metrology.]

Laser Metrology

Recently Published

Sanford, N.A., Malone, K.J., Aust, J.A., and Larson, D.R., **Rare-Earth-Doped Waveguide Devices**, Proceedings of the OSA Annual Meeting, Albuquerque, New Mexico, September 20-25, 1992, p. 57.

Rare-earth-doped integrated optic waveguide lasers have been demonstrated in glass, $LiNbO_3$ and other host materials. This technology offers a variety of new components that include diode-pumped amplifiers and lasers. The planar geometry is particularly attractive because selective doping permits the integration of passive and active devices on the same substrate and it is also compatible with pumping by laser diodes. Ion exchanged channel waveguides have been demonstrated to lase near 1060 nm and 1320 nm in Nd-doped silicate and Nd-doped phosphate glass, respectively. Nd-doped waveguide lasers have also been fabricated by chemical vapor deposition; Er-doped waveguide lasers have been similarly fabricated. Y-branch splitters with gain at 1060 nm have been reported in Nd-doped silicate glass waveguides. Ion implantation has been used to form waveguides in Nd-doped YAG and Nd-doped GGG. Nd and Er-doped $LiNbO_3$ waveguide lasers operating near 1060 nm and 1550 nm, respectively, have also been reported. Attempts have been made to demonstrate visible upconversion lasing in Er-doped $LiNbO_3$ and $LiTaO_3$ waveguides. We review the status of this technology and also highlight some of the more promising applications.
[Contact: Norman A. Sanford, (303) 497-5239]

Optical Fiber Metrology

Released for Publication

Franzen, D.L., **Lightwave Standards Development at NIST**, to be published in the Proceedings of the DoD Fiber Optics and Photonics Conference, McLean, Virginia, March 21-24, 1994.

Standards are being developed at the National Institute of Standards and Technology to support the following parameters of interest to the lightwave communication industry: optical fiber geometry, optical fiber chromatic dispersion, absolute optical power, high-speed detector frequency response, and wavelength.
[Contact: Douglas L. Franzen, (303) 497-3346]

Gilbert, S.L., and Patrick, H., **Comparison of UV-Induced Fluorescence and Bragg Grating Growth in Optical Fiber**, to be published in the Proceedings of the Conference on Lasers and Electro-Optics, Anaheim, California, May 8-13, 1994.

We have measured the time dependence of the 400-nm fluorescence of Ge-doped optical fiber illuminated with continuous-wave 244-nm light. Our results differ from previous measurements that used pulsed 242-nm light.
[Sarah L. Gilbert, (303) 497-3120]

Optical Fiber/Waveguide Sensors

Released for Publication

Rochford, K.B., and Day, G.W., **Polarization Dependence of Response Functions in 3 x 3 Sagnac Optical Fiber Current Sensors**.

The response functions of a lossless Sagnac optical fiber current sensor based on a 3 x 3 coupler fundamentally depend on the polarization state of light entering the coupler, even for systems with zero linear birefringence. For this system, the desired response functions, sinusoids separated by 120° phase shifts, are obtained only for circularly polarized light. The response functions for linearly

polarized and depolarized inputs are sinusoids separated by 180° and yield zero-slope small-signal responses; in addition, two outputs are degenerate, so the responses are similar to those observed in 2 x 2 systems. Thus, 3 x 3 couplers offer no advantage over 2 x 2 systems for linearly polarized input light. This result increases system complexity in that polarization control optics are required to supply the proper polarization.
[Contact: Kent B. Rochford, (303) 497-5170]

Integrated Optics — [formerly Electro-Optic Metrology.]

Released for Publication

Franzen, D.L., **Lightwave Standards Development at NIST**, to be published in the Proceedings of the DoD Fiber Optics and Photonics Conference, McLean, Virginia, March 21-24, 1994.

[See Optical Fiber Metrology.]

Gallawa, R.L., Kumar, A., and Weisshaar, A., **Coupling of Modes and Loss on Tapered Optical Waveguides**, to be published in the Proceedings of the International Photonics Research Conference, San Francisco, California, February 17-19, 1994.

Tapered dielectric waveguides have been analyzed using a variety of methods including the coupled mode theory, a step tapered configuration, a method that uses a ray-optics model, and the beam propagation method. We also use a step taper approach, approximating the smooth taper with a series of discrete steps. Our method accounts for the interaction between modes and is capable of tracking the propagation through the taper by using an expansion of the field on each side of the step; we use basis functions that are known to approximate the field very accurately. Integration is avoided in evaluating the coupling efficiency across the step.
[Contact: Robert L. Gallawa, (303) 497-3761]

Hickernell, R.K., Christensen, D.H., Pellegrino, J.G., Wang, J., and Leburton, J.P., **Determination of the Complex Refractive Index of Individual Quantum Wells from Distributed Reflectance**.

We investigated the measurement of the complex refractive index of individual quantum wells by reflectance spectroscopy. Placing the wells at half-wavelength spacing to cause resonant feedback produces an order-of-magnitude increase in measurement sensitive over that of nonresonant structures. Quantum well dispersive and absorptive effects on reflectance can be differentiated in certain spectral regions. Experimental data confirm a theoretical model of refractive index and absorption for quantum wells of GaAs $Al_{0.2}Ga_{0.8}As$ in the region of the well bandgap.
[Contact: Robert K. Hickernell, (303) 497-3455]

Kumar, A., and Gallawa, R.L., **Bent Rectangular Core Waveguides: An Accurate Perturbation Approach**.

We report on a simple method to evaluate accurately the effective indices of various quasi-modes of a bent rectangular core waveguide. The correct dielectric constant in the corner regions, which is ignored in earlier methods, is taken into account through a first-order perturbation approach. At small bend curvatures and low V-values, the contribution of the corner regions to the effective index is much larger than that due to the bending itself. By ignoring this contribution, the error encountered in the calculations of bending induced phase shifts of the two modes increases with increase in curvature.
[Contact: Robert L. Gallawa, (303) 497-3761]

Kumar, A., Gallawa, R.L., and Goyal, I.C., **Propagation Characteristics of Bent Planar Optical Waveguides**, to be published in the Proceedings of the International Photonics Research Conference, San Francisco, California, January 17-19, 1994.

Modal characteristics of bent dual-mode planar waveguides are obtained. The fundamental and the second modes show surprisingly different bending-induced phase changes at high V-values.
[Contact: Robert L. Gallawa, (303) 497-3761]

Schaafsma, D.T., Christensen, D.H., Hickernell, R.K., and Pellegrino, J.G., **Comparative Photoluminescence Measurement and Simulation of Vertical-Cavity Semiconductor Laser Structures**, to be published in the

Proceedings of the Materials Research Society Conference, Boston, Massachusetts, November 29—December 3, 1993.

The increasing manufacturing and research activity in the area of vertical-cavity surface-emitting lasers (VCSELs) has underscored the need for complete and accurate characterization tools. We have shown previously that comparisons of reflectance spectroscopy, double-crystal X-ray diffractometry, and electron microscopy, aided by simulation tools, can determine the mirror and cavity layer thicknesses to within 0.8% agreement. Since most VCSEL devices use quantum wells (QWs) as their active media and the above techniques yield little direct information about the nanoscale properties of the QWs, the remaining metrology must be filled in by measurements such as photoluminescence (PL). Yet, since the semiconductor layers used to create the mirrors of the microcavity distort surface-normal QW and alloy emission spectra, direct interpretation of these results can lead to incorrect characterization of these materials. Depending on the detuning of the QW emission from the cavity resonance, the apparent surface-normal emission peak can differ from the actual peak by several nanometers. We present a comparison of PL data for various VCSEL and distributed quantum well structures taken with the pump beam (and the collection path) in two different configurations: normal to the surface of the sample (NPL); and perpendicular to a cross-section of the epitaxial layers (XPL). We elucidate a potential method for transforming between the perturbed NPL spectra and the non-perturbed XPL spectra and attempt to evaluate the sensitivity of this method to various measurement as well as material parameters. These simulations are well-suited to wide parametric variations of the dispersion curves for the complex dielectric constant of the materials, the pump field distribution, and the depth profile of the gain medium.
[Contact: David T. Schaafsma, (303) 497-7281]

Integrated Optics — [formerly Electro-Optic Metrology]

Recently Published

Kumar, A., and R.L. Gallawa, **Bending-Induced Phase Shifts in Dual-Mode Planar Optical Waveguides**, Optics Letters, Vol. 18, No. 17, pp. 1415-1417 (September 1, 1993).

We examine the manner in which the effective index for each of the two modes of a bent dual-mode planar waveguide changes with curvature. We find that the bending-induced changes in the effective indices depend strongly on core-cladding index contrast and the value of *V*. For waveguides with large contrast, the changes in effective indices are such that the change in the phase difference between the modes is positive (or negative) at large (or small) values of *V*. The change becomes zero at a *V*-value that depends on the waveguide parameters and curvature. If the index contrast is small, the bending-induced phase difference may change sign with increase in curvature. This might help in ultimately explaining the bipolar phase shift seen in a recent experiment. The results of our study can be used to increase or decrease the bending sensitivity of dual-mode optical-waveguide sensors and devices.
[Contact: Robert L. Gallawa, (303) 497-3761]

Patrick, H., and Gilbert, S.L., **Growth of Bragg Gratings Produced by Continuous-Wave Ultraviolet Light in Optical Fiber**, Optics Letters, Vol. 18, No. 18, pp. 1484-1486 (September 15, 1983).

We have written Bragg gratings of as much as 94% reflectance in germanium-doped optical fiber by two-beam interference of 244-nm continuous-wave UV light. We measured grating reflectance as a function of exposure time for UV light intensities ranging from 1.5 to 47 W/cm^2. The observed dependence of index modulation on time and intensity does not agree with the predictions of a model based on depletion of a defect population by one-photon absorption.
[Contact: Heather Patrick, (303) 497-6353]

Complex System Testing

Released for Publication

Koffman, A.D., and Souders, T.M., **Application of the NIST Testing Strategies to a Multirange Instrument**, to be published in the Proceedings of the Measurement Science Conference, Pasadena, California, January 27-28, 1994.

A new modeling and test point reduction technique for analog and mixed-signal devices has been developed at the National Institute of Standards and Technology. This technique has been applied as a case study to the Fluke 792A Thermal Transfer Standard for potential use in testing and calibration. An empirical model is formulated using complete test data from many devices collected from several production runs. The model is then algebraically reduced using singular value decomposition and QR decomposition. Once the final reduced model is obtained, it is used to test devices which are measured only at a reduced set of test points. The model allows accurate prediction of device behavior at all other test points. Techniques for optimal model size selection are discussed. Device modeling results are presented and compared to complete test data.
[Contact: Andrew D. Koffman, (301) 975-4518]

ELECTRICAL SYSTEMS

Power Systems Metrology

Released for Publication

Stricklett, K.L., and Sununu, C., **Refraction of Light by Graded Birefringent Media**, to be published in the Proceedings of the 1993 Conference on Electrical Insulation and Dielectric Phenomena, Pocono Manor, Pennsylvania, October 17-20, 1993.

To date, proposals to use the Kerr effect to map divergent electric fields have not considered refraction of light in the graded potential. Spatial variation of the strength or direction of the field will produce nonuniform refractive indices, and significant refraction of light in regions of high divergence may distort the final image and introduce an error in the field measurement. Experimental evidence for this effect is presented, and its implications to optical field mapping are discussed.
[Contact: Kenneth L. Stricklett, (303) 497-3955]

Power Systems Metrology

Recently Published

Anderson, W.E., **Research for Electric Energy Systems - An Annual Report**, NISTIR 5268 (December 1992).

This report documents the technical progress of two investigations. The first investigation is concerned with the measurement of magnetic fields in support of epidemiological and *in-vitro* studies of biological field effects. During 1992, the derivation of equations which predict differences between the average magnetic flux density using circular coil probes and the flux density at the center of the probe, assuming a dipole magnetic field, were completed. The information gained using these equations allows the determination of measurement uncertainty due to probe size when magnetic fields from many electrical appliances are characterized. Consultations with various state and federal organizations and the development of standards related to electric and magnetic field measurements continue. The second investigation is concerned with two different activities related to compressed-gas insulated high-voltage systems: 1) the measurement of dissociative electron attachment cross sections and negative ion production in S_2F_{10}, S_2OF_{10}, and $S_2O_2F_{10}$, and 2) Monte-Carlo simulations of ac-generated partial-discharge pulses that can occur in SF_6- insulated power systems and can be sources of gas decomposition.
[Contact: William E. Anderson, (301) 975-2432]

Van Brunt, R.J., von Glahn, P., and Las, T., **Partial Discharge-Induced Aging of Cast Epoxies and Related Nonstationary Behavior of the Discharge**, Proceedings of the 1993 Annual Report of the IEEE Conference on Electrical Insulation and Dielectric Phenomena, Pocono Manor, Pennsylvania, October 17-20, 1993, pp. 455-461.

Measurements were made of the time dependences of positive and negative integrated-charge distributions for ac-generated pulsating partial discharge (PD) in point-to-dielectric gaps where the dielectric material was cast epoxy either with or without an aluminum oxide filler. Other statistical characteristics of the PD were measured such as pulse-phase distributions. The dielectric surface resistivity was measured before and after exposure to PD. For epoxy with filler, the PD statistical characteristics changed significantly during times when there was a corresponding decrease in local

surface resistivity. For example, the positive PD pulses were observed to cease after a time that is inversely proportional to the frequency of the applied voltage. Partial discharge from epoxy without filler exhibited a much more stationary behavior. The connection between changes in surface resistivity and changes in stochastic behavior are explained using a Monte Carlo simulation.
[Contact: Richard J. Van Brunt, (303) 975-2425]

Magnetic Materials and Measurements

Released for Publication

Oti, J.O., Rice, P., and Russek, S., **Antiferromagnetically Coupled Dual-Layer Magnetic Force Microscope Tips**.

We describe a magnetic force microscope tip designed from dual-layer magnetic films of antiferromagnetically coupled magnetic layers. A previously described micromagnetic model of conventional single-layer tips is expanded to a dual-layer model and used to analyze the new tip. In contrast to single-layer tips, the magnetic domains of dual-layer tips are impervious to fringing fields of the specimen, and the tip stray fields are greatly reduced, thus minimizing the likelihood of the erasure of the sample magnetization. These properties of dual-layer tips should lead to improved resolution of magnetic force microscopy images.
[Contact: John O. Oti, (303) 497-5557]

Oti, J.O., Russek, S.E., and Sanders, S.C., **Magnetic and Magnetoresistive Properties of Inhomogeneous Magnetic Dual-Layer Films**.

Magnetic and magnetoresistive properties of sputtered Co alloy dual-layer films are compared with micromagnetic simulations. The simulations elucidate the details of the switching behavior of the dual-layer films as a function of the interlayer exchange and magnetostatic interactions. The simulations have led to a conceptual understanding of the coercive field splitting caused by the interlayer interactions. A calculation of the anisotropic magnetoresistance (AMR) has been included in the simulations. The AMR provides a second independent macroscopic quantity (in addition to the average magnetization) which can be measured and compared with the micromagnetic simulations. The AMR is more sensitive to the micromagnetic structure perpendicular to the applied field and is a better test of the accuracy of the micromagnetic model. The simulations fit well to the measured AMR data on CoNi-Cr-CoNi dual-layers.
[Contact: John O. Oti, (303) 497-5557]

Rice, P., and Moreland, J., **Flexible Diaphragm Force Microscope**.

A flexible polyamide diaphragm was used in place of the usual cantilever for atomic force microscopy. Images of hard disk surface features, using this technique, are presented demonstrating the practicality of the method.
[Contact: Paul Rice, (303) 497-3841]

Magnetic Materials and Measurements

Recently Published

Moreland, J., **Tunneling Stabilized Magnetic-Force Microscopy**, Proceedings of the 51st Annual Meeting of the Microscopy Society of America, Cincinatti, Ohio, August 2-6, 1993, pp. 1034-1035.

Magnetic force microscopy (MFM) can be done by making a simple change in conventional scanning tunneling microscopy (STM) where the usual rigid STM tip is replaced with a flexible magnetic tip. STM images acquired this way show both the topography and the magnetic forces acting on the flexible tip. The z-motion of the STM piezo tube scanner flexes the tip to balance the magnetic force so that the end of the tip remains a fixed tunneling distance from the sample surface. We present a review of some "tunneling-stabilized" MFM (TSMFM) images showing magnetic bit tracks on a hard disk, Bloch wall domains in garnet films, and flux patterns in high-T_c superconductor films. The image resolution of TSMFM is routinely 0.1 μm using Au-coated magnetic tips cut from Ni or Fe films. Recent results show that a TSMFM resolution of less than 40 nm is possible with micromachined cantilevers coated with a very thin Au-Fe bilayer.
[Contact: John Moreland, (303) 497-3641]

Moreland, J., Rice, P., and Wadas, A., **Magnetic**

Force Microscopy of Flux In Superconductors, Proceedings of the 1993 International Workshop on Superconductivity, "Characterization of High Temperature Superconductors: Structures and Properties of Surfaces and Interfaces," Hokkaido, Japan, June 28—July 1, 1993, pp. 77-80.

We are developing a novel form of magnetic force microscopy (MFM) which is well suited for low-temperature imaging of magnetic flux lines penetrating superconductors. This method is based on standard scanning tunneling microscopy where the usual rigid tunneling tip is replaced with a flexible magnetic tip. We present a discussion of the interpretations of these images which includes theoretical aspects of MFM of flux lines in superconductors and experimental details regarding MFM which we believe are critical for flux imaging. [Contact: John Moreland, (303) 497-3641]

Superconductors

Released for Publication

Aized, D., Haddad, J.W., Joshi, C.H., and Goodrich, L.F., **HTSC Voltage-Current Simulator - A Tool for Comparing the Accuracy of Critical Current Measurement Methods**, to be published in the Proceedings of the Thirteenth International Conference on Magnet Technology, Vancouver, British Columbia, September 20-24, 1993.

A passive voltage-current simulator has been developed by the National Institute of Standards and Technology (NIST) to compare the accuracy of different methods used for measurement of critical current and power-law behavior of high-temperature superconductors (HTSC). In the present study, four different measurement and data analysis systems used for electric characterization of HTSC coils at the American Superconductor Corporation are compared. The measurements were compared with those carried out at NIST. Different measurement techniques, methods of calculating critical current, and index values are discussed. The V-1 simulator is believed to be an advancement towards defining the standards for critical current measurements ensuring the traceability of results at different test facilities.
[Contact: Loren F. Goodrich, (303) 497-3143]

Ekin, J.W., Bray, S.L., Lutgen, C.L., and Bahn, W.L., **Electromechanical Characteristics of Superconductors for DOE Fusion Applications**, to be published as NISTIR 5013.

The electrical performance of many superconducting materials is strongly dependent on mechanical load. This report presents electromechanical data on a broad range of high-magnetic-field superconductors. The conductors that were studied fall into three general categories: candidate conductors, experimental conductors, and reference conductors. Research on candidate conductors for fusion applications provides screening data for superconductor selection as well as engineering data for magnet design and performance analysis. The effect of axial tensile strain on critical-current density was measured for several Nb_3Sn candidate conductors including the US-DPC (United States Demonstration Poloidal Coil) cable strand and an ITER (International Thermonuclear Experimental Reactor) candidate conductor. Also, data are presented on promising experimental superconductors that have strong potential for fusion applications. Axial strain measurements were made on a V_3Ga tape conductor that has good performance at magnetic fields up to 20 T. Axial strain data are also presented for three experimental Nb_3Sn conductors that contain dispersion-hardened copper reinforcement for increased tensile strength. Finally, electromechanical characteristics were measured for three different Nb_3Sn reference conductors from the first and second VAMAS (Versailles Project on Advanced Materials and Standards) international Nb_3Sn critical-current round robins. Published papers containing key results, including the first measurement of the transverse stress effect in Nb_3Sn, the effect of stress concentration at cable-strand crossovers, and electromechanical characteristics of Nb_3Al, are included throughout the report.
[Contact: John W. Ekin, (303) 497-5448]

Goldfarb, R.B., and Itoh, K., **Reduction of Interfilament Contact Loss in Nb_3Sn Superconductor Wires**.

Interfilament contact in Nb_3Sn wires made by the internal-tin-diffusion process causes excess hysteresis loss beyond the intrinsic magnetic

hysteresis loss of the filaments. In analogy with eddy-current and proximity-effect coupling losses, the excess contact loss can be reduced by decreasing the twist-pitch length of the filaments in the wire. One consequence of interfilament contact is that volume magnetization measurements are strongly dependent on sample length below about one twist pitch. We define a characteristic length whose reciprocal is equal to the sum of the reciprocals of the sample length and the twist pitch. Hysteresis loss is a universal function of characteristic length for different sample lengths and twist pitches. We discuss several experimental parameters for the magnetic determination of hysteresis loss.
[Contact: Ronald B. Goldfarb, (303) 497-3650]

Russek, S.E., Sanders, S.C., Roshko, A., and Ekin, J.W., **Surface Degradation of Superconducting $YBa_2Cu_3O_{7-\delta}$ Thin Films**.

[See Cryoelectronic Metrology.]

Superconductors

Recently Published

Booi, P.A., Livingston, C.A., and Benz, S.P., **Intrinsic Stress in dc Sputtered Niobium**, IEEE Transactions on Applied Superconductivity, Vol. 3, No. 2, pp. 3029-3031 (June 1993).

[See Cryoelectronic Metrology.]

Chen, D.-X., Goldfarb, R.B., Cross, R.W., and Sanchez, A., **Surface Barrier and Lower Critical Field in $YBa_2Cu_3O_{7-\delta}$ Superconductors**, Physical Review B, Vol. 48, No. 9, pp. 6426-6430 (September 1993).

The fields for first vortex entry and last vortex exit, H_1 and H_2, and the lower critical field H_{c1} for a grain-aligned, sintered $YBa_2Cu_3O_{7-\delta}$ superconductor have been determined from saturated magnetic-hysteresis loops using an extended critical-state model. For fields oriented along the grain c axis, H_1 increases with decreasing temperature, showing an upturn below 50 K, whereas H_2 remains small and positive, in general agreement with the theory of Bean-Livingston surface barriers. H_{c1} has a Bardeen-Cooper-Schrieffer temperature dependence above 50 K, but it rises at low temperatures. For fields oriented in the ab plane, H_{c1} has a similar temperature dependence, but surface barriers are not evident in the magnetization.
[Contact: Ronald B. Goldfarb, (303) 497-3650]

Coffey, M.W., **Transverse Thermomagnetic Effects In the Mixed State and Lower Critical Field of High-T_c Superconductors**, Physical Review B, Vol. 48, No. 13, pp. 9767-9771, (October 1993).

Transverse thermomagnetic effects (Ettingshausen, Nernst effects) are discussed for a variety of phenomenological models of high-T_c and other layered superconductors. The use of the temperature-dependent vortex-line energy in determining the transport entropy is stressed, leading to predictions and possibilities for additional experiments. The dynamics of both Abrikosov and Josephson vortices is considered.
[Contact: Mark W. Coffey, (303) 497-3703]

Ekin, J.W., **Preparation of Low Resistivity Contacts for High-T_c Superconductors**, in Processing and Properties of High-T_c Superconductors, Vol. 1, Chapter 9 (World Scientific Publishing Company, Singapore, 1993), pp. 371-407.

[See Cryoelectronic Metrology.]

Goodrich, L.F., Srivastava, A.N., Yuyama, M., and Wada, H., **n-Value and Second Derivative of the SuperconductorVoltage-CurrentCharacteristic**, IEEE Transactions on Applied Superconductivity, Vol. 3, No. 1, pp. 1265-1268 (March 1993).

We studied the n-value ($V \propto I^n$) and second derivative (d^2V/dI^2) of the voltage-current curve of high- and low-temperature superconductors and superconductor simulators. We used these parameters for diagnosing problems with sample heating and data acquisition, and as indicators of the superconducting-to-normal state transition. The superconductor simulator may be useful in testing the measurement system integrity and reducing measurement variability since its characteristics are highly repeatable.
[Contact: Loren F. Goodrich, (303) 497-3143]

Ishida, T., Goldfarb, R.B., Okayasu, S., Kazumata, Y., Franz, J., Arndt, T., and Schauer, W., **Harmonic and Static Susceptibilities of $YBa_2Cu_3O_7$**, Materials Science Forum, Vol. 137-139, pp. 103-131 (1993).

Intergranular properties of the sintered superconductor $YBa_2Cu_3O_7$ have been studied in terms of complex harmonic magnetic susceptibility $\chi_n = \chi'_n - i\chi''_n$ (n integer) as well as dc susceptibility χ_{dc}. As functions of temperature T, χ'_1 and χ''_1 depend on both the ac magnetic field amplitude H_{ac} and the magnitude of a superimposed dc field H_{dc}. Only odd-harmonic susceptibilities are observed below the critical temperature, T_c, for zero H_{dc} while both odd and even harmonics are observed for nonzero H_{dc}. With T constant, odd-harmonic susceptibilities are even functions of H_{dc}, whereas even-harmonic susceptibilities are odd functions of H_{dc}. Experimental intergranular characteristics of χ'_1 and χ''_1 are in good agreement with theoretical predictions from a simplified Kim model of magnetization. In contrast, even-harmonic susceptibilities measured for a $GdBa_2Cu_3O_7$ thin film and an $YBa_2Cu_3O_7$ single crystal are not prominent due to missing weak links, whereas odd-harmonic susceptibilities are remarkable. A survey of several models for the harmonic response of superconductors is presented. The dc susceptibility curve for the zero-field-cooled $YBa_2Cu_3O_7$ sample, $\chi_{ZFC}(T)$, has a two-step structure arising from intra- and inter-granular components, similar to χ'_1. The dc susceptibility measured upon warming, $\chi_{FCW}(T)$, shows a negative peak near T_c for the sample cooled rapidly in small dc fields. The dc susceptibility measured upon cooling, $\chi_{FCC}(T)$, does not show a peak. A negative peak is not seen in measurements on a powdered sample. The negative peak can be explained by intergranular flux depinning upon warming.
[Contact: Ronald B. Goldfarb, (303) 497-3650]

Moreland, J., **Tunneling Spectroscopy of Thallium-Based High Temperature Superconductors**, Chapter in Thallium-Based High-Temperature Superconductors, A.M. Hermann and J.V. Yakhmi, Eds. (Marcel Dekker, Inc., New York, NY, 1994), pp. 569-577.

[See Cryoelectronic Metrology.]

Peterson, R.L., **An Analysis of the Impact on U.S. Industry of the NIST/Boulder Superconductivity Programs: An Interim Study**, NISTIR 5012 (November 1993).

[See Cryoelectronic Metrology.]

Shi, D., Wang, Z., Sengupta, S., Smith, M., Goodrich, L.F., Dou, S.X., Liu, H.K., and Guo, Y.C., **Critical Current Density Irreversibility Line and Flux Creep Activation Energy In Silver-Sheathed $Bi_2Sr_2Ca_3Cu_3O_x$ Superconducting Tapes**, IEEE Transactions on Applied Superconductivity, Vol. 3, No. 1, pp. 1194-1196 (March 1993).

Transport data, magnetic hysteresis, and flux creep activation energy experimental results are presented for silver-sheathed high-T_c $Bi_2Sr_2Ca_2Cu_3O_x$ superconducting tapes. The 110-K superconducting phase was formed by lead doping in a Bi-Sr-Ca-Cu-O system. The transport critical current density was measured at 4.0 K to be 0.7×10^5 A/cm^2 (the corresponding critical current is 74 A) at zero field and 1.6×10^4 A/cm^2 at 12 T for $H \| ab$. Excellent grain alignment in the a-b plane was achieved by a short-melting method, which considerably improved the critical current density and irreversibility line. Flux creep activation energy as a function of current is obtained based on the magnetic relaxation measurements.
[Contact: Loren F. Goodrich, (303) 497-3143]

ELECTROMAGNETIC INTERFERENCE

Conducted EMI

Recently Published

Lai, J.-S., and Martzloff, F.D., **Coordinating Cascaded Surge Protection Devices: High-Low Versus Low-High**, IEEE Transactions on Industry Applications, Vol. 29, No. 4, pp. 680-687 (July/August 1993). [Also published in the Conference Record of the IEEE/IAS Annual Meeting, Dearborn, Michigan, October 1-4, 1991, Vol. II, pp. 1812-1819.]

Cascading surge-protection devices located at the service entrance of a building and near the sensitive equipment are intended to ensure that each device

shares the surge stress in an optimum manner to achieve reliable protection of equipment against surges impinging from the utility supply. However, depending on the relative clamping voltages of the two devices, their separation distance, and the waveform of the impinging surges, the coordination may or may not be effective. The paper provides computations with experimental verification of the energy deposited in the devices for a matrix of combinations of these three parameters. Results show coordination to be effective for some combinations and ineffective for some others which is a finding that should reconcile contradictory conclusions reported by different authors making different assumptions. From these results, improved coordination can be developed by application standards writers and system designers.
[Contact: François D. Martzloff, (301) 975-2409]

ELECTROMAGNETIC INTERFERENCE

Radiated EMI

Released for Publication

Hill, D.A., Cavcey, K.H., and Johnk, R., **Crosstalk Between Microstrip Transmission Lines**.

[See Microwave and Millimeter-Wave Metrology.]

Hill, D.A., Ma, M.T., Ondrejka, A.R., Riddle, B.F., Crawford, M.L., and Johnk, R., **Aperture Excitation of Electrically Large, Lossy Cavities**.

We present a theory based on power balance for aperture excitation of electrically large, lossy cavities. The theory yields expressions for shielding effectiveness, cavity Q, and cavity time constant. In shielding effectiveness calculations, the incident field can be either a single plane wave or a uniformly random field to model reverberation chamber or random field illumination. The Q theory includes wall loss, absorption by lossy objects within the cavity, aperture leakage, and power received by antennas within the cavity. Extensive measurements of shielding effectiveness, cavity Q, and cavity time constant were made on a rectangular cavity, and good agreement with theory was obtained for frequencies from 1 to 18 GHz.
[Contact: David A. Hill, (303) 497-3472]

Kanda, M., **Methodology for Electromagnetic Interference Measurements**.

Establishing standards for electromagnetic field measurements is a multifaceted endeavor which requires measurements made (1) in anechoic chambers, (2) at open-sites, and (3) within guided-wave structures, and the means to transfer these measurements from one situation to another. The underlying principles of these standard measurements and transfer standards fall into one of two categories: (1) measurements or (2) theoretical modeling. In the former, a parameter or a set of parameters is measured, while in the latter, a parameter is calculated employing established physical and mathematical principles. In the following discussion, the three measurement topics and field transfer standards mentioned above are discussed, with the guided-wave structures being restricted to the TEM cell. Throughout the discussion the interplay between measured quantities and predicted (modeled) quantities will be seen. The frequencies considered here range from 10 kHz to 40 GHz (and upward) and are determined by our ability to make an actual measurement and the restrictions imposed by rigorous theoretical analysis of a given model.
[Contact: Motohisa Kanda, (303) 497-5320]

Randa, J.P., Gilliland, D., Gjertson, W., Lauber, W., and McInerney, M., **Catalogue of Electromagnetic Environment Measurements, 30-300 HZ**.

The IEEE Electromagnetic Compatibility Society's Technical Committee on Electromagnetic Environments (TC-3) has undertaken a long-term project to compile an inventory or catalogue of published measurements of electromagnetic environments. The frequency spectrum has been divided into tractable bands which will be considered one at a time. We have now completed the 30- to 300-Hz band. This paper presents the resulting bibliography, along with a brief overview of what has been measured.
[Contact: James P. Randa, (303) 497-3150]

LAW ENFORCEMENT STANDARDS

Released for Publication

Calvano, N.J., and Frank, D.E., **Autoloading Pistols for Police Officers**.

This standard establishes performance requirements and test methods for pistols to be used by law enforcement officers. This standard is a revision of and supersedes NIJ Standard-0112.01 dated May 1989. This revision adds 10-mm Auto and 40 S&W to the standard. The standard is intended for use in assessing the acceptability of new or reissue autoloading pistols. This standard does not address specific safety devices, full or partial magazine release, pistol shot group size, accuracy, or sights, nor does this standard address service life (endurance testing).
[Contact: Nicholas J. Calvano, (301) 975-2755]

VIDEO TECHNOLOGY

Released for Publication

Kelley, E.F., Field, B.F., and Fenimore, C., **Nonlinear Color Transformations in Real Time Using a Video Supercomputer**, to be published in the Proceedings of the Color Imaging Conference, Phoenix, Arizona, November 7-11, 1993.

Investigations of the effects of color transformations used for video displays are often hampered by the inability to see the effects of these changes in real time for a variety of input signals. Using a video supercomputer, the Princeton Engine, the effects of a parametric nonlinear color transformation can be shown in real time.
[Contact: Edward F. Kelley, (301) 975-3842]

ADDITIONAL INFORMATION

Lists of Publications

Smith, A.J., **Metrology for Electromagnetic Technology: A Bibliography of NIST Publications**, NISTIR 5008 (September 1993).

This bibliography lists the publications of the personnel of the Electromagnetic Technology Division of NIST during the period from January 1970 through publication of this report. A few earlier references that are directly related to the present work of the Division are also included.
[Contact: Annie Smith, (303) 497-3678]

Lyons, R.M., and Gibson, K.A., **A Bibliography of the NIST Electromagnetic Fields Division Publications**, NISTIR 5009 (September 1993).

This bibliography lists publications by the staff of the National Institute of Standards and Technology's Electromagnetic Fields Division for the period from January 1970 through July 1993. Selected earlier publications from the Division's predecessor organizations are included.
[Contact: Kathryn A. Gibson, (303) 497-3132]

Meiselman, B., **Electrical and Electronic Metrology: A Bibliography of NIST Electricity Division's Publications, NIST List of Publications 94** (January 1994).

This bibliography covers publications of the Electricity Division, Electronics and Electrical Engineering, Laboratory, NIST, and of its predecessor sections for the period January 1968 to December 1993. A brief description of the Division's technical program is given in the introduction.
[Contact: Katherine H. Magruder, (301) 975-2401]

Walters, E.J., **Semiconductor Measurement Technology, 1990-1992, NIST List of Publications 103** (April 1993).

The bibliography provides information on technology transfer in the field of microelectronics at NIST for the calendar years 1990 and 1992. Publications from groups specializing in semiconductor electronics are included, along with NIST-wide research now coordinated by the NIST Office of Microelectronics Programs which was established in 1991. Indices by topic area and by author are provided. Earlier reports of work performed during the period from 1962 through December 1989 are provided in NIST List of Publications 72.
[Contact: E. Jane Walters, (301) 975-2050]

Availability of *Measurements for Competitiveness in Electronics* [First Edition], NISTIR 4583 (April 1993).

This document is the successor to NISTIR 90-4260, *Emerging Technologies in Electronics ...and their Measurement Needs* [Second Edition]. The new *Measurements for Competitiveness in Electronics* identifies the measurement needs that are most critical to U.S. competitiveness, that would have the

highest economic impact if met, and that are the most difficult for the broad range of individual companies to address. The document has two primary purposes: (1) to show the close relationship between U.S. measurement infrastructure and U.S. competitiveness, and show why improved measurement capability offers such high economic leverage and (2) to provide a consensus on the principal measurement needs affecting U.S. competitiveness, as the basis for an *action plan* to meet those needs and to improve U.S. competitiveness.

Copies of this document are available as Order No. PB93-160588 from the National Technical Information Service, 5285 Port Royal Road, Springfield, VA 22161, at (800) 553-6847 or (703) 487-4650.

Abstract – Measurements are used to determine the values of hundreds of important quantities in the electronics industry. Representative quantities are the widths of the interconnections within semiconductor integrated circuits, the attenuation of lightwaves in optical fibers, and the signal power from microwave satellite antennas. Measurement capability is a fundamental tool used to build the nation's high-technology products. As such, it is part of the national infrastructure for the realization of these products.

Measurement capability is critical to research and development, manufacturing, marketplace entry, and after-sales support of products. Thus, measurement capability affects the performance, quality, reliability, and cost of products. The result of this pervasive impact is that the level of U.S. measurement capability places an upper limit on the competitiveness of U.S. products.

At present, U.S. industry is experiencing a major shortfall in the measurement capability needed for competitiveness in electronic products. This document identifies the measurement needs that are most critical to U.S. competitiveness, that would have the highest economic impact if met, and that are the most difficult for the broad range of individual companies to address. The measurement needs are reviewed for nine important fields of electronics, including semiconductors, magnetics, superconductors, microwaves, lasers, optical-fiber communications, optical-fiber sensors, video, and electromagnetic compatibility. These fields of electronics underlie more than $300 billion of electronic and electrical products manufactured in the U.S. each year.

This assessment provides the framework for an action plan to correct the shortfall in U.S. measurement capability in electronics and to advance U.S. competitiveness.

Guide – The compiler of the document provided an introductory guide to its organization and content. Because EEEL believes that a number of *TPB* readers will be interested in the information presented in the various chapters, the contents of this guide are reproduced below (page numbers of chapter summaries are included to provide a measure of the extent of the treatment):

This document contains 12 chapters, divided into two groups. The first three chapters are introductory in nature and are relevant to all of the following chapters. The remaining nine chapters address individual fields of electronic technology. Each chapter begins with a two-page summary that provides ready access to the major points made in the chapter. These short summaries are found on the pages identified below. By selecting from these summaries, you can quickly access information on the subjects of most interest to you.

Introductory Information – Chapter 1, Role of Measurements in Competitiveness (page 3); Chapter 2, NIST's Role in Measurements (page 21); Chapter 3, Overview of U.S. Electronics and Electrical-Equipment Industries (page 31).

These three chapters introduce the subject of measurements and provide an overview of the products of the U.S. electronics and electrical-equipment industries.

Chapter 1, **Role of Measurements in Competitiveness**, shows why measurements are a fundamental part of the infrastructure of the nation. Chapter 1 also sets measurements in the context of the many other important factors that affect competitiveness.

Chapter 2, **NIST's Role in Measurements**, indicates the circumstances under which Government assistance to industry in the development of

measurement capability is appropriate in pursuit of a strengthened national economy.

Chapter 3, **Overview of U.S. Electronics and Electrical-Equipment Industries**, introduces these industries through an overview of their major product lines. This chapter shows the various ways in which the products of these industries are commonly classified and how those classifications relate to the structure of this document.

Fields of Technology -- Chapter 4, Semiconductors (page 53); Chapter 5, Magnetics (page 95); Chapter 6, Superconductors (page 129); Chapter 7, Microwaves (page 147); Chapter 8, Lasers (page 183); Chapter 9, Optical-Fiber Communications (page 217); Chapter 10, Optical-Fiber Sensors (page 303); Chapter 11, Video (page 339); Chapter 12, Electromagnetic Compatibility (page 381).

Each of these chapters contains four basic types of information:

Technology Review: The field of technology is reviewed to highlight and explain the special capabilities that make the technology important. This review introduces the technical concepts that are necessary for understanding the sections that follow.

World Markets and U.S. Competitiveness: The economic significance of the field of technology is highlighted through use of national and international market data for major products that employ the technology. Available information on the U.S. competitiveness is described.

Goals of U.S. Industry for Competitiveness: The goals that U.S. industry is pursuing to improve its competitiveness are discussed so that they can be related to requirements for new measurement capability supportive of the goals.

Measurement Needs: The new measurement capability that U.S. industry will need to enable it to achieve its goals is described. This discussion emphasizes measurement capability that is needed widely in U.S. industry, that will have high economic impact if provided, and that is beyond the resources of the broad range of individual U.S. companies to provide.

[While the assessment of measurement needs in this document is wide ranging, not every field of technology important to the electronic and electrical-equipment industries has been covered. NIST plans to expand this assessment in future editions to include additional fields.]

The order in which chapters appear is intentional: the technologies on which most other technologies depend are introduced first. Thus, the chapter on semiconductors appears first because most electronic technologies depend on semiconductor materials. In contrast, the chapter on video is located near the end because it depends on nearly every other technology discussed earlier.

Chapters 4, 5, and 6 of this document describe the measurement needs arising from three important materials technologies that underlie current and emerging electronic and electrical products. These chapters also describe the measurement needs of components and equipment based on these materials and not discussed separately in other chapters.

Chapter 4, **Semiconductors**, addresses both silicon and compound semiconductors and their use in components, including individual (discrete) electronic and optoelectronic devices and integrated circuits. Semiconductor components are central to all modern electronic products from consumer products to supercomputers.

Chapter 5, **Magnetics**, focuses on both magnetic materials and the components made from them. Magnetic materials are second in importance only to semiconductor materials for electronic products and play a central role in electrical products. This chapter also addresses the measurement needs of selected equipment critically dependent on magnetic materials, including magnetic information storage equipment, electrical power transformers, and others.

Chapter 6, **Superconductors**, examines superconductor materials and addresses both present and emerging applications of these materials in electronic and electrical products.

Chapters 7 through 11 describe the measurement needs associated with selected technologies of

importance to U.S. competitiveness for current and emerging products.

Chapter 7, **Microwaves**, describes the highest-information-capacity radio technology. Microwave electronics provide the basis for modern and emerging wireless communications systems and radar systems. Included are new personal communications services with both local and worldwide access, intelligent vehicle-highway systems, and advanced audio and video broadcasting systems, among others.

Chapter 8, **Lasers**, addressed the single most important component for emerging lightwave systems used for manufacturing, medicine, communications, printing, environmental sensing, and many other applications.

Chapter 9, **Optical-Fiber Communications**, describes the highest-information-capacity cable technology. It provides the basis for national and international information highways of unprecedented performance and broad economic impact. Optical-fiber systems will be linked with microwave systems to interconnect mobile and portable users and to backup cable systems.

Chapter 10, **Optical-Fiber Sensors**, focuses on an emerging class of sensors that offers outstanding performance for a broad spectrum of applications in manufacturing, aerospace, medicine, electrical power, and other areas.

Chapter 11, **Video**, emphasizes advanced, high-performance systems, such as high-definition television, which offer, for the first time, simultaneous access to high-resolution, smooth motion, and great color depth. The chapter notes the potential of full-power implementations of video technology in interactive networked environments. The chapter contains a special focus on flat-panel displays.

Chapter 12, **Electromagnetic Compatibility**, describes the special challenges that the U.S. faces in maintaining electromagnetic compatibility among the many new products of electronic and electrical technologies. Such compatibility is essential if the full potential of all of the above technologies is to be realized without debilitating mutual interference.

Appendices -- The three appendices provide definitions of the U.S. electronics and electrical-equipment industries. These definitions were used in preparing much of the economic information in the report.

Appendix 1 describes the Standard Industrial Classification System that the U.S. Government uses for collecting data about U.S. industry. This appendix also lists publications in which the U.S. Government reports data on U.S. shipments.

Appendix 2 provides a definition of the U.S. electronics industry in terms of the Standard Industrial Classification System.

Appendix 3 provides a definition of the U.S. electrical-equipment industry in terms of the Standard Industrial Classification System.

1994/1995 Calendar of Events

April 28, 1994 (Hudson, Massachusetts)

Ion Implant Users Group Meeting. This NIST-sponsored meeting will be held at the facilities of Digital Equipment in Hudson, Massachusetts. Among the topics to be discussed is Large Area Implantation.
[Contact: John Albers, (301) 975-2075]

June 8-10, 1994 (near Windsor, U.K.)

IEEE/CHMT Workshop on MCM and VLSI Packaging Techniques and Manufacturing Technologies. Sponsored by IEEE/CHMT Society and NIST, this Workshop will be held in cooperation with the European Communities DGXIII-A. The main topics of the Workshop will be the design and implementation of first-level electronic packaging and the technologies, materials, and equipment for the manufacture of multichip modules (MCM) and single-chip packages.
[Contact: George G. Harman, (301) 975-2097]

June 14-17, 1994 (Boulder, Colorado)

Computer Modeling of Optical Waveguides and Components: A Hands-On Workshop. The purpose of this Workshop, sponsored by NIST, is to disseminate computer modeling tools for fiber and

integrated optics waveguides and to discuss and demonstrate methods of understanding engineering parameters of optical waveguides.
[Contact: Robert L. Gallawa, (303) 497-3761]

June 27-July 1, 1994 (Boulder, Colorado)

Conference on Precision Electromagnetic Measurements. In sponsorship with the IEEE Instrumentation and Measurement Society and Union Radio Scientifique Internationale, NIST will be holding the biennial meeting of CPEM in Boulder, Colorado. Topics to be discussed include: advanced instrumentation including new sensors and measurement methods; automated measurement methods; dielectric and antenna measurements; direct current and low-frequency measurements; fundamental constants and special standards; laser, optical fiber, and optical electronic measurements; RF, microwave, and millimeter-wave measurements; superconducting and other low-temperature measurements; and time and frequency measurements. CPEM '94 is extended to five days to provide for added special sessions on the fundamental constants.
[Contact: Gwen E. Bennett, (303) 497-3295]

September 13-15, 1994 (Boulder, Colorado)

Symposium on Optical Fiber Measurements. Sponsored by the IEEE Lasers & Electro-Optics Society, the Optical Society of America, and NIST, the Symposium will provide a forum for reporting the results of recent measurement research in the area of lightwave communications, including optical fibers.
[Contact: Douglas L. Franzen, (303) 497-3346]

January 30—February 2, 1995 (Gaithersburg, Maryland) — *(PLEASE NOTE NEW DATE.)*

International Workshop on Semiconductor Materials Characterization: Present Status and Future Needs. Papers will be presented in all relevant fields of interest to materials characterization in semiconductor device manufacturing, growth, processing, diagnostics, in-situ, real-time control and monitoring, etc. All relevant semiconductor materials will be addressed: Group IV elements, Group III-V compounds, Group II-VI compounds, IV-VI compounds, and others. The Workshop is sponsored by the Advanced Research Projects Agency (ARPA), SEMATECH, and NIST. Other co-sponsors are expected.
[Contact: David G. Seiler, (301) 975-2074]

EEEL Sponsors

National Institute of Standards and Technology
Executive Office of the President
U.S. Air Force
  Hanscom Field; Newark Air Force Station; Strategic Defense Systems Command
U.S. Army
  Fort Belvoir; Redstone Arsenal; Combined Army/Navy/Air Force (CCG); Materials & Mechanics Research Strategic Defense Command
Department of Defense
  Advanced Research Projects Agency; Defense Nuclear Agency; National Security Agency
Department of Energy
  Building Energy R&D; Energy Systems Research; Fusion Energy; Basic Energy Sciences; Oak Ridge National Lab
Department of Justice
  Law Enforcement Assistance Administration; Federal Bureau of Investigation
U.S. Navy
  Seal Beach; Naval Sea Systems Command; Office of Naval Research; Naval Aviation Depot; Naval Air Systems Command; Naval Air Engineering Center; Naval Surface Warfare Center; Naval Ocean Systems Center;
National Aeronautics and Space Administration
  NASA Headquarters; Goddard Space Flight Center; Lewis Research Center
Department of Transportation
  National Highway Traffic Safety Administration; Federal Aviation Administration
Tennessee Valley Authority
MIMIC Consortium
Various Federal Government Agencies

NIST Silicon Resistivity SRMs

In response to needs of the semiconductor industry, NIST's Semiconductor Electronics Division provides silicon bulk resistivity Standard Reference Materials (SRMs) through the NIST Standard Reference Materials Program. A new class of resistivity SRMs is being introduced to respond better to users' requirements.

The first NIST (then NBS) resistivity SRMs were fabricated from crystal 50 mm (2 in) in diameter. These wafers represented various combinations of crystal growth process, crystallographic orientation, and doping, each combination chosen to give the best expected wafer uniformity for a given resistivity level. Each wafer in every set was individually measured and certified. Some of these sets are still available until the supply is exhausted (see table).

The Division is now certifying single-wafer resistivity standards at approximately the same resistivity values as were available in the earlier sets. These new SRMs are fabricated from crystal 100 mm in diameter, intended to provide improved compatibility with newer end-use instrumentation. In response to user comments, the new SRMs will be more uniform in both thickness and resistivity, will have reduced uncertainty of certified value due to use of an improved certification procedure using a four-point probe, and will be measured and certified at additional measurement sites for better characterization of wafer uniformity at its core. The additional measurements needed to qualify the improved SRMs will make them more expensive on a per-wafer basis than the earlier sets.

NIST SILICON BULK RESISTIVITY STANDARD REFERENCE MATERIALS

DATE UPDATED: 4 FEBRUARY 1994

NOMINAL RESISTIVITY (ohm · cm)	OLD SRMs	AVAILABILITY	NEW SRMs	ANTICIPATED AVAILABILITY
0.01	1523 (one of set of two wafers)	limited supply	2541	to be announced
0.1	1521 (one of set of two wafers)	limited supply	2542	to be announced
1	1523 (one of set of two wafers)	limited supply	2543	to be announced
10	1521 (one of set of two wafers)	limited supply	2544	early in calendar year 1994
25	1522	set of three wafers no longer available	2545	to be announced
75	1522		2546 (100)	to be announced
180	1522		2547 (200)	early in calendar year 1994

The above table will be updated in future issues to reflect changes in availability. Every effort will be made to provide accurate statements of availability; NIST sells SRMS on an as-available basis. For technical information, contact James R. Ehrstein, (301) 975-2060; for ordering information, call the Standard Reference Materials Program Domestic Sales Office: (301) 975-6776.

INTERNATIONAL WORKSHOP ON
Semiconductor Characterization: Present Status and Future Needs

NOTE NEW DATE

January 30 - February 2, 1995
Gaithersburg, Maryland, U.S.A.

Sponsors

The Advanced Research Projects Agency, National Institute of Standards and Technology, and SEMATECH. Other expected co-sponsors: Air Force Office of Scientific Research, Department of Energy, Office of Naval Research, and the National Science Foundation.

Purpose and Goals of the Workshop

Semiconductors form the backbone of all modern-day microelectronic and optoelectronic devices. Semiconductor characterization has proven to be fundamental for the advancement of semiconductor technology. A comprehensive "world-class" workshop dedicated to giving critical reviews of the most important semiconductor characterization techniques that are useful to the semiconductor industry is envisioned. Because of the increasing importance of in-line and in-situ characterization methods, a strong emphasis will be placed on ascertaining their present status and future needs.

The purpose of this workshop is to bring together scientists and engineers interested in all aspects of characterization (research, development, manufacturing, diagnostics...): chemical and physical, electrical, optical, in-situ, and real-time control and monitoring.

The workshop goals are: (1) to provide a forum in which measurements of current and future interest to the semiconductor industry can be reviewed, discussed, critiqued, and summarized; (2) to demonstrate and review important applications for diagnostics, manufacturing, and in-situ monitoring and control in real-time environments; and (3) to act as an important stimulus for new progress in the field by providing new perspectives.

Scope of the Workshop

Papers are solicited in all relevant fields of interest to characterization in semiconductor device manufacturing, growth, processing, diagnostics, in-situ, real-time control and monitoring, etc. All relevant semiconductor materials will be addressed: Group IV elements (Si, etc.), Group III-V compounds (GaAs, InP, etc.), Group II-VI compounds (ZnSe, HgCdTe, etc.), IV-VI compounds (PbTe, etc.), and others. Heavy emphasis will be placed on invited papers that provide up-to-date critical reviews that discuss and evaluate the science and technology of the major techniques or areas. Recent developments of novel measurement methods will also be considered.

For technical information, contact: Dr. David G. Seiler, NIST, A305 Technology Bldg., Gaithersburg, MD 20899-0001, USA, Telephone: 301/975-2081, Fax: 301/948-4081, email: seiler@sed.eeel.nist.gov

The National Institute of Standards and Technology

NIST Standard Reference Materials (SRMs) are used by thousands of companies to calibrate their equipment

NIST photomask SRMs help reduce linewidth measurement errors by a factor of 10 and save manufacturers over $30 million annually

NIST research in electromigration is saving manufacturers over $26 million and has contributed to a new thrust in building-in reliability

NIST research improved production yield of high reliability devices by factors of 2 to 35

NIST developed a tester that characterizes the breakdown of semiconductor power devices without destroying them

NIST is developing test structures and test methods for nanometer overlay metrology

NIST is developing new optical measurement tools for advanced semiconductor manufacturing

NIST research works.

Find out how NIST can help you.
See us at SEMICON/West '94
July 19-21, 1994, San Francisco, Calif.

Hall 4, Booth 5722
MOSCONE CENTER

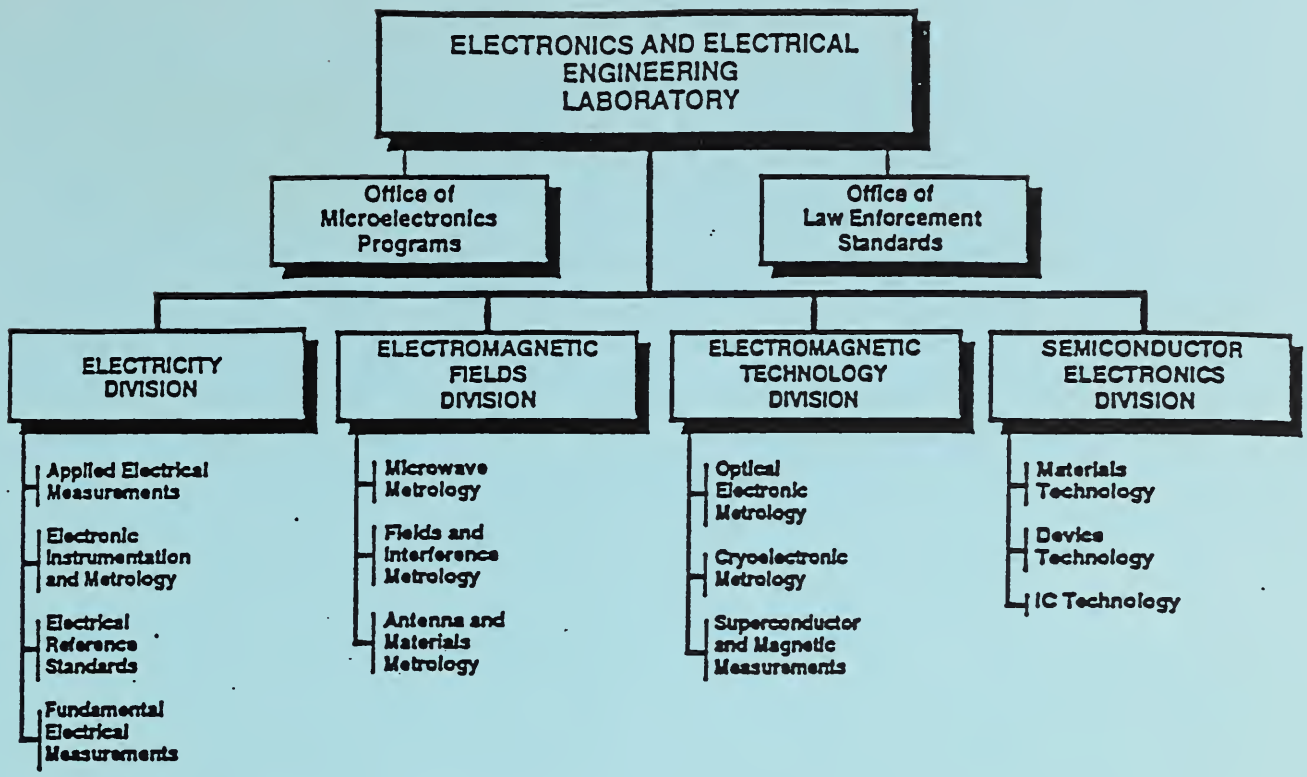

KEY CONTACTS

Laboratory Headquarters (810)	Director, Judson, C. French (301) 975-2220
	Deputy Director, Dr. Robert E. Hebner (301) 975-2220
Office of Microelectronics Programs	Director, Mr. Robert I. Scace (301) 975-2485
Office of Law Enforcement Standards	Acting Director, Dr. Daniel E. Frank (301) 975-2757
Electricity Division (811)	Acting Chief, Dr. Alan H. Cookson (301) 975-2400
Semiconductor Electronics Division (812)	Chief, Mr. Frank F. Oettinger (301) 975-2054
Electromagnetic Fields Division (813)	Chief, Mr. Allen C. Newell (303) 497-3131
Electromagnetic Technology Division (814)	Acting Chief, Dr. Richard E. Harris (303) 497-3776

INFORMATION:

For additional information on the Electronics and Electrical Engineering Laboratory, write or call:

Electronics and Electrical Engineering Laboratory
National Institute of Standards and Technology
Metrology Building, Room B-358
Gaithersburg, MD 20899
Telephone: (301) 975-2220